

Numerical Explorations of Cake Baking
Using the Nonlinear Heat Equation

Rebecca L. Wilkinson

A Thesis Submitted to the
University of North Carolina Wilmington in Partial Fulfillment
of the Requirements for the Degree of
Master of Science

Department of Mathematics and Statistics

University of North Carolina Wilmington

2008

Approved by

Advisory Committee

Gabriel Lugo

Mark Lammers

Russell Herman

Chair

Accepted by

Dean, Graduate School

TABLE OF CONTENTS

ABSTRACT	iii
ACKNOWLEDGMENTS	iv
1 INTRODUCTION	1
2 EXACT SOLUTIONS	4
2.1 Rectangular Cakes	4
2.2 Cylindrical Cakes	10
3 CONSTANT D VALUES	17
4 FINITE DIFFERENCE SCHEME	26
5 NUMERICAL SOLUTIONS	30
5.1 Piecewise Constant D Case	31
5.2 Linear Approximation of D Values	34
5.3 Non-Linear Approximation of D Values	37
5.4 Comparison of Diffusion Models	40
6 CONCLUSIONS	44
REFERENCES	46
APPENDIX	47
A. Diffusion	47
B. Besselzeros	48
C. Numerical Solutions	50
D. Non-Constant Plots	55

ABSTRACT

Much can be said about the culinary aspects of cake baking. How much of and which types of ingredients are used to determine the flavor of the cake. However, is flavor the only ingredient for taste? Does a dry, crumbling cake still satisfy the pallet? One can control the flavor of the batter, but once it is placed in the oven for baking, what determines the consistency of the finished dessert? We consider a simple model of the actual baking process which is based on the diffusion equation

$$\frac{\partial T}{\partial t} = \nabla \cdot (D \nabla T), \quad (1)$$

where D is the heat diffusivity of the batter and T is the temperature of the cake at time t . We begin with this model and numerically investigate solutions for various cake geometries while also looking at the effects of varying the heat diffusivity over space and time.

ACKNOWLEDGMENTS

First of all I would like to thank my committee, Dr.'s Herman, Lugo and Lammers, for their knowledge and guidance throughout this process. Dr. Herman has especially dedicated much of his free time to assist with the expanse of equations now known as Bessel's equation, as well as in writing and correcting countless MATLAB[®] codes. I have greatly appreciated all of their time and effort and am honored to have had the opportunity to work with such an elite group of individuals.

I would also not be where I am today if not for the remaining members of the University of North Carolina Wilmington Mathematics and Statistics Department. They have not only helped me further my mathematics education, but have also provided me with valuable teaching and personal learning experiences for which I will be forever grateful. I had the pleasure of working closely with Mrs. Spike and would like to take this time to thank her for all of the wonderful advice and resources she has allowed me access to over the years. I contribute much of my teaching methods to her and so many of the outstanding professors with which I have had the pleasure of working.

Last, but certainly not least, to my friends and family: I would not be *who* I am today without your love and support and am eternally indebted to you all. You have been my guiding light throughout everything that has seemed to arise during this inevitably lengthy process. Thank you for believing in me and being my determination along the way. I dedicate this to you.

1 INTRODUCTION

Numerous research has been devoted to the baking process. From casting metals, to food safety, firing pottery, to creating the desired crust on bread, consistent temperature development plays a signature roll in the outcome of many different products. Too much or too little heat can result in problems as severe as structural instability or sickness, or as minor as discoloration or superficial burning. However, as seemingly replaceable as a cracked vase or defective steel rod may be, someone is inevitably charged for the time, money and effort to do so. In a growing economy, millions of dollars are spent trying to simulate and model fundamental processes in order to perfect and standardize results. Whether it be in determining the ideal temperature environment to produce consistent products of the various natures listed above or the cooking time required to ensure safe food quality, the ability to numerically translate a production process can help save both the time and the money spent on extensive research.

Dealing with the culinary baking process, cake baking in particular, the model we intend to use has previously been studied in the development of crust on bread in both domestic and factory settings. Depending on the type of bread desired, a specific crust-crumbs ratio is needed. An evaporation front has been described as what separates the crust from the crumb of the bread, which moves towards the center as the water evaporates, creating the crust along the areas of dough closest to the pan [1]. More specific to our topic, the paper by Dr. Olszewski explores the possibility of predicting baking times of various cakes given the initial dimensions, baking time, and heat diffusivity of previously baked cakes [2]. His simple, initial model assumes the heat diffusivity of the batter is constant. However, noting that there is more water evaporation from the top, uncovered layer of the batter leads to an alternate study of ways in which the rate of diffusion changes throughout the

baking process.

In this thesis we would like to:

1. Numerically investigate the results Dr. Olszewski found when changing the dimensions of the cake pan [2];
2. Numerically study the effects of varying the diffusion coefficients in space and time as the cake bakes;

We first wish to discuss the heat equation used to model the baking process and note the assumptions that have been made in its development. In general, we begin with Fourier's law of heat conduction [5] which states that the heat flux throughout a region per unit time is proportional to the rate of change of the temperature across the region:

$$\phi = -K_0 \frac{\partial T}{\partial x},$$

where ϕ represents heat flux and K_0 is the thermal conductivity of the material [5]. (The negative sign indicates the idea that heat flows from areas of higher temperatures to those of lower temperatures which, in coordination with Newton's Law of Heating and Cooling, could also be the basis for a similar model of the baking process.) Since cakes comprise of both depth and height, this three-dimensional case then represents the change in temperature as the gradient of the temperature, or

$$\phi = -K_0 \nabla T. \tag{2}$$

We must also take into account that energy must be conserved across the boundary, meaning the rate of change in heat energy over time must be proportional to the change in energy across the boundary. This equates to

$$\frac{\partial e}{\partial t} = -\nabla \cdot \phi + Q, \tag{3}$$

where Q represents any internal source and $e = c\rho u$ is the heat energy (c is the specific heat and ρ the density of the batter) [5]. For simplicity, we let $Q = 0$ and assume no heat is internally created due to radiation. Also assuming the specific heat is independent of time and that density changes only with volume, we have $e(r, z, t) = c(r, z)\rho(r, z)u(r, z, t)$. When we substitute this and Equation (2) into Equation (3), we get

$$c\rho\frac{\partial T}{\partial t} = \nabla \cdot (K_0\nabla T). \quad (4)$$

Separating our temporal and spatial derivatives, and assuming c and ρ are approximately constant, we define our three-dimensional heat equation as

$$\frac{\partial T}{\partial t} = \nabla \cdot (D\nabla T), \quad (5)$$

for $D = \frac{K_0(r,z)}{c\rho}$.

We will first explore D as a constant rate, changing Equation (5) into

$$\frac{\partial T}{\partial t} = D\nabla^2 T,$$

and then discuss why this is an inadequate assumption in modeling the cake baking process.

2 EXACT SOLUTIONS

2.1 Rectangular Cakes

We will begin our review of the known solutions of the heat equation in three-dimensional Cartesian space ($0 \leq x \leq W, 0 \leq y \leq L, 0 \leq z \leq H$). For example, this could correspond to $13'' \times 9'' \times 2''$ baking pan. Assuming that the diffusion parameter D is constant, we begin with the heat equation in 3D:

$$\frac{\partial T}{\partial t} = D\nabla^2 T. \quad (6)$$

We will need to specify initial and boundary conditions. Let T_i be the initial batter temperature, and write the initial condition as

$$T(x, y, z, 0) = T_i.$$

We choose the boundary conditions to be fixed at the oven temperature T_b ,

$$T(0, y, z, t) = T(W, y, z, t) = T_b,$$

$$T(x, 0, z, t) = T(x, L, z, t) = T_b,$$

$$T(x, y, 0, t) = T(x, y, H, t) = T_b.$$

We will assume throughout the paper that $T_i = 80^\circ\text{F}$ and $T_b = 350^\circ\text{F}$.

It is easier to solve Equation (2) when there are homogeneous boundary conditions. In this case we can use the method of separation of variables [5]. So, subtracting the temperature of the oven from all temperatures involved and defining $u(x, y, z, t) = T(x, y, z, t) - T_b$, the heat equation becomes

$$\frac{\partial u}{\partial t} = D\nabla^2 u \quad (7)$$

with initial condition

$$u(x, y, z, 0) = T_i - T_b$$

and boundary conditions

$$u(0, y, z, t) = u(W, y, z, t) = 0,$$

$$u(x, 0, z, t) = u(x, L, z, t) = 0,$$

$$u(x, y, 0, t) = u(x, y, H, t) = 0.$$

Using the method of separation of variables, we seek solutions of the form

$$u(x, y, z, t) = X(x)Y(y)Z(z)G(t). \quad (8)$$

Substituting (8) into the left and right hand sides of (7), we attain

$$\frac{\partial u}{\partial t} = XYZG' \quad \text{and} \quad \nabla^2 u = X''YZG + XY''ZG + XYZ''G.$$

Therefore,

$$XYZG' = D(X''YZG + XY''ZG + XYZ''G). \quad (9)$$

By dividing both sides of (9) by $DXYZG$ we get

$$\frac{1}{D} \frac{G'}{G} = \frac{X''}{X} + \frac{Y''}{Y} + \frac{Z''}{Z}. \quad (10)$$

We know the only way for the function of time (t) on the left to be equal to a function of the variables (x, y, z) on the right is for them to equal a constant. Anticipating an exponential decay in time, we choose our constant to be $-\lambda^2$. (We could have just as easily chosen to use $-\lambda$ but would have to later restrict $\lambda > 0$ to ensure

the quantity $-\lambda$ was in fact negative.) The need of the negative sign will become apparent momentarily.

Setting Equation (10) equal to $-\lambda^2$, we get the following

$$\frac{1}{D} \frac{G'}{G} = -\lambda^2 \quad \text{and} \quad \frac{X''}{X} + \frac{Y''}{Y} + \frac{Z''}{Z} = -\lambda^2. \quad (11)$$

Thus,

$$G' + D\lambda^2 G = 0 \quad \text{and} \quad \frac{X''}{X} = -\frac{Y''}{Y} - \frac{Z''}{Z} - \lambda^2 = -\mu^2. \quad (12)$$

Reasoning as before, we have chosen another strategically arbitrary constant, $-\mu^2$, to further separate our spatial variables. Likewise, we can continue the process using $-\nu^2$ and $-\kappa^2$. This yields

$$\frac{Y''}{Y} = -\frac{Z''}{Z} - \lambda^2 + \mu^2 = -\nu^2, \quad (13)$$

$$\frac{Z''}{Z} = -\lambda^2 + \mu^2 + \nu^2 = -\kappa^2. \quad (14)$$

From Equations (12)-(14) we get the following set of ODE's

$$\begin{aligned} G' + D\lambda^2 G &= 0, \\ X'' + \mu^2 X &= 0, \\ Y'' + \nu^2 Y &= 0, \\ Z'' + \kappa^2 Z &= 0, \end{aligned} \quad (15)$$

where $\lambda^2 = \mu^2 + \nu^2 + \kappa^2$ from Equation (14).

The solution of the first-order linear differential equation in time is of the form $G = Ae^{-\lambda^2 Dt}$, where $\lambda^2 = \mu^2 + \nu^2 + \kappa^2$ from before and A is some constant. Since we are discussing heat flow throughout a cake, we do not expect solutions that grow

exponentially over time, hence one insight into our choosing a negative separation constant.

The general solution of the differential equation $X'' + \mu^2 X = 0$ is

$$X = c_1 \cos \mu x + c_2 \sin \mu x, \quad (16)$$

where c_1 and c_2 are arbitrary constants.

Applying our homogeneous boundary conditions, the first, $X(0) = 0$, implies $c_1 = 0$. The second boundary condition, $X(W) = 0$, then yields $c_2 \sin \mu W = 0$. Since $c_2 = 0$ would give a trivial solution, we look at the case(s) where $\sin \mu W = 0$. We know this occurs when μW equals some multiple of π , or

$$\mu_m = \frac{m\pi}{W}, \quad m = 1, 2, \dots \quad (17)$$

Again, from experience, we know that only positive eigenvalues, μ , yield nontrivial solutions when satisfying the boundary conditions. So, substituting (17) back into the right half of Equation (16), and given the same work has been shown for $Y(y)$ and $Z(z)$, we get fundamental solutions

$$\begin{aligned} X_m(x) &= \sin\left(\frac{m\pi x}{W}\right) \\ Y_n(y) &= \sin\left(\frac{n\pi y}{L}\right) \\ Z_\ell(z) &= \sin\left(\frac{\ell\pi z}{H}\right). \end{aligned} \quad m, n, \ell = 1, 2, \dots \quad (18)$$

Thus, our product solutions for u are

$$u_{mnl}(x, y, z, t) = \sin(\mu_m x) \sin(\nu_n y) \sin(\kappa_\ell z) e^{-\lambda_{mnl}^2 Dt},$$

for

$$\lambda_{mnl}^2 = \mu_m^2 + \nu_n^2 + \kappa_\ell^2 = \left(\frac{m\pi}{W}\right)^2 + \left(\frac{n\pi}{L}\right)^2 + \left(\frac{\ell\pi}{H}\right)^2,$$

$m, n, \ell = 1, 2, \dots$. A linear superposition of these product solutions is also a solution, so we write

$$u(x, y, z, t) = \sum_{m=1}^{\infty} \sum_{n=1}^{\infty} \sum_{\ell=1}^{\infty} A_{mnl} \sin(\mu_m x) \sin(\nu_n y) \sin(\kappa_\ell z) e^{-\lambda_{mnl}^2 D t}, \quad (19)$$

where the A_{mnl} 's are arbitrary constants. To determine the A_{mnl} 's we use our initial condition $u(x, y, z, 0) = T_i - T_b$. We find

$$T_i - T_b = \sum_{m=1}^{\infty} \sum_{n=1}^{\infty} \sum_{\ell=1}^{\infty} A_{mnl} \sin(\mu_m x) \sin(\nu_n y) \sin(\kappa_\ell z). \quad (20)$$

This is a triple Fourier sine series. If we let $b_m(y, z) = \sum_{n=1}^{\infty} \sum_{\ell=1}^{\infty} A_{mnl} \sin(\nu_n y) \sin(\kappa_\ell z)$, Equation (20) becomes

$$T_i - T_b = \sum_{m=1}^{\infty} b_m(y, z) \sin(\mu_m x), \quad (21)$$

a simple sine series. Multiplying both sides by $\sin(\mu_k x)$ and then integrating over the interval, we get

$$\int_0^W (T_i - T_b) \sin(\mu_k x) dx = \sum_{m=1}^{\infty} \int_0^W b_m(y, z) \sin(\mu_m x) \sin(\mu_k x) dx.$$

By orthogonality of sine functions, the integral's vanish unless $k = m$ so only one term in the sum remains,

$$\frac{2}{W} \int_0^W (T_i - T_b) \sin(\mu_m x) dx = b_m(y, z).$$

Using the same technique for the remaining sine series in Equation (20) gives

$$\begin{aligned}
A_{mnl} &= \frac{2}{W} \frac{2}{L} \frac{2}{H} \int_0^H \int_0^L \int_0^W (T_i - T_b) \sin(\mu_m x) \sin(\nu_n y) \sin(\kappa_\ell z) dx dy dz \\
&= (T_i - T_b) \frac{8}{\pi^3} \left[\frac{\cos(\frac{m\pi x}{W})}{m} \right]_0^W \left[\frac{\cos(\frac{n\pi y}{L})}{n} \right]_0^L \left[\frac{\cos(\frac{\ell\pi z}{H})}{\ell} \right]_0^H \\
&= (T_i - T_b) \frac{8}{\pi^3} \left[\frac{\cos m\pi - 1}{m} \right] \left[\frac{\cos n\pi - 1}{n} \right] \left[\frac{\cos \ell\pi - 1}{\ell} \right] \\
&= (T_i - T_b) \frac{8}{\pi^3} \begin{cases} 0, & \text{for at least one } m, n, \ell \text{ even,} \\ \left[\frac{-2}{m} \right] \left[\frac{-2}{n} \right] \left[\frac{-2}{\ell} \right], & \text{for } m, n, \ell \text{ all odd.} \end{cases}
\end{aligned}$$

Since only the odd multiples yield non-zero A_{mnl} we let $m = 2m' - 1$, $n = 2n' - 1$, and $\ell = 2\ell' - 1$. Thus

$$A_{mnl} = \frac{-64(T_i - T_b)}{(2m' - 1)(2n' - 1)(2\ell' - 1)\pi^3}.$$

Substituting this result into Equation (20) and dropping the primes, we find

$$u(x, y, z, t) = \frac{-64(T_i - T_b)}{\pi^3} \sum_{m=1}^{\infty} \sum_{n=1}^{\infty} \sum_{\ell=1}^{\infty} \frac{\sin(\hat{\mu}_m x) \sin(\hat{\nu}_n y) \sin(\hat{\kappa}_\ell z) e^{-\hat{\lambda}_{mnl}^2 Dt}}{(2m-1)(2n-1)(2\ell-1)},$$

where

$$\hat{\lambda}_{mnl}^2 = \hat{\mu}_m^2 + \hat{\nu}_n^2 + \hat{\kappa}_\ell^2 = \left(\frac{(2m-1)\pi}{W} \right)^2 + \left(\frac{(2n-1)\pi}{L} \right)^2 + \left(\frac{(2\ell-1)\pi}{H} \right)^2$$

for $m, n, \ell = 1, 2, \dots$

Recalling $T(x, y, z, t) = u(x, y, z, t) - T_b$,

$$T(x, y, z, t) = T_b - \frac{64(T_i - T_b)}{\pi^3} \sum_{m=1}^{\infty} \sum_{n=1}^{\infty} \sum_{\ell=1}^{\infty} \frac{\sin(\hat{\mu}_m x) \sin(\hat{\nu}_n y) \sin(\hat{\kappa}_\ell z) e^{-\hat{\lambda}_{mnl}^2 Dt}}{(2m-1)(2n-1)(2\ell-1)}.$$

By programming these solutions into MATLAB[®], we are able to visually represent the temperature development throughout the cake during the baking

process. In Figure 1, vertical slices are taken at the indicated positions and times indicated until half the length of a for $13'' \times 9'' \times 2''$ cake due to symmetry.

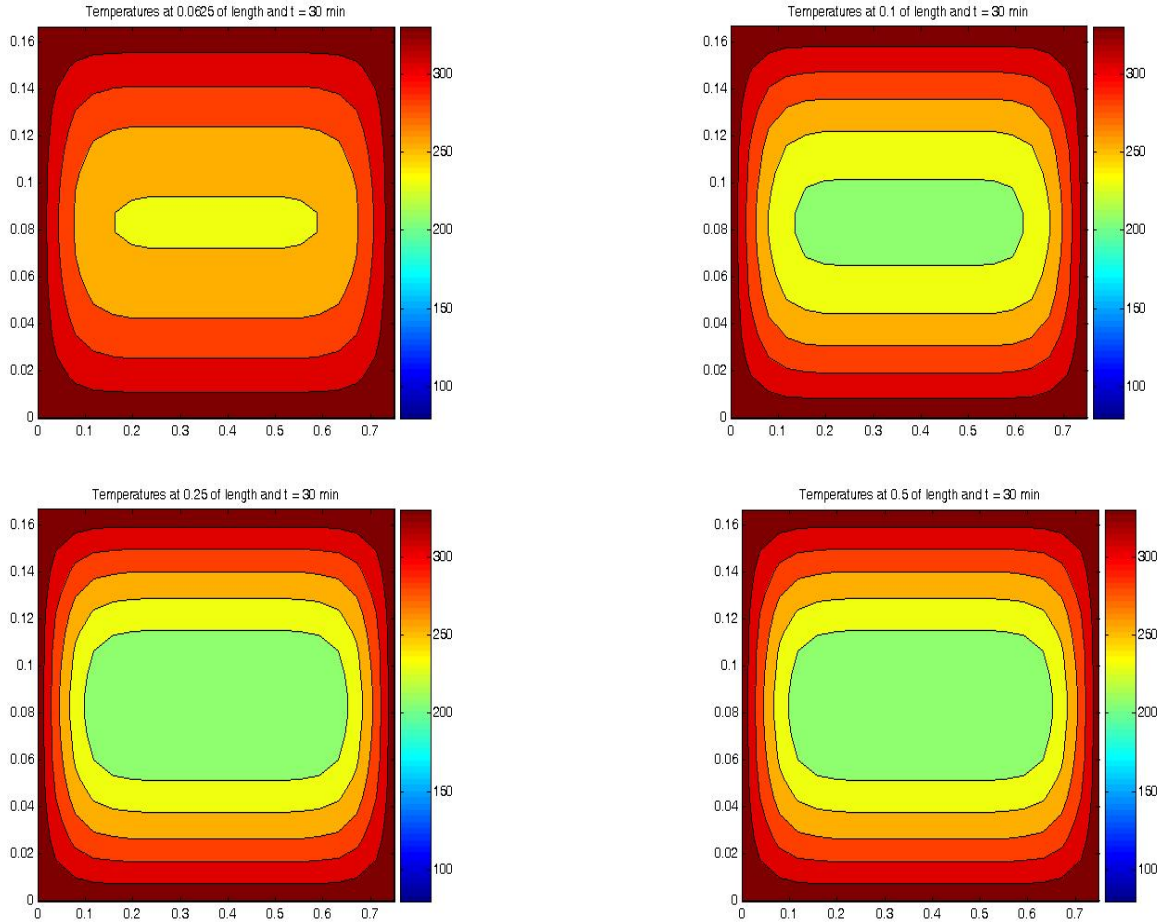


Figure 1: Temperature development throughout a $13'' \times 9'' \times 2''$ cake shown as vertical slices at the indicated length. Width horizontal and height vertical are given in feet.

2.2 Cylindrical Cakes

Now that we have reviewed the process of solving the three-dimensional heat equation in rectangular coordinates, we would like to apply the same method to determine the known solutions in cylindrical coordinates (r, θ, z) . We assume $T = T(r, z, t)$ is independent of θ due to symmetry. We begin as before

with nonhomogeneous boundary conditions and thus use the same substitution of $u(r, z, t) = T(r, z, t) - T_b$ to obtain

$$\frac{\partial u}{\partial t} = D\nabla^2 u = D \left(\frac{1}{r} \frac{\partial}{\partial r} \left(r \frac{\partial u}{\partial r} \right) + \frac{\partial^2 u}{\partial z^2} \right), \quad (22)$$

where $0 \leq r \leq a$ and $0 \leq z \leq Z$. The initial condition is

$$u(r, z, 0) = T_i - T_b,$$

and the homogeneous boundary conditions are

$$\begin{aligned} u(a, z, t) &= 0, \\ u(r, 0, t) &= u(r, Z, t) = 0, \end{aligned}$$

where $r = a$ corresponds to the side of the cake and $z = 0, Z$ the bottom and top, respectively. Again, we seek solutions of the form $u(r, z, t) = R(r)H(z)G(t)$. Separation of variables leads to

$$\frac{1}{D} \frac{G'}{G} = \frac{1}{r} \frac{1}{R} \frac{d}{dr} (rR') + \frac{H''}{H}. \quad (23)$$

Choosing λ as the separation constant, we get

$$G' - D\lambda G = 0, \quad (24)$$

and

$$\frac{1}{r} \frac{1}{R} \frac{d}{dr} (rR') = -\frac{H''}{H} + \lambda. \quad (25)$$

Since negative eigenvalues yield the oscillatory solutions we expect, we continue as before by setting both sides of Equation (25) equal to $-\mu^2$. Simplifying accordingly,

we have

$$\frac{d}{dr}(rR') + r\mu^2 R = 0 \quad (26)$$

and

$$\frac{H''}{H} = \lambda + \mu^2 \equiv -\nu^2,$$

or

$$H'' + \nu^2 H = 0. \quad (27)$$

Here $\lambda = -(\mu^2 + \nu^2)$.

Equation (24) has the solution $G(t) = Ae^{\lambda Dt}$. Again, since we do not expect unbounded solutions over time, we would normally need to restrict $\lambda < 0$. However, this has already been established since $\lambda = -(\mu^2 + \nu^2) < 0$.

Equation (27) subject to the fixed homogeneous boundary conditions is satisfied by

$$H_n(z) = \sin\left(\frac{n\pi z}{Z}\right), n = 1, 2, 3, \dots,$$

where $\nu = \frac{n\pi}{Z}$. Recalling that only odd terms arise in the Fourier sine series coefficients of the constant initial condition, we proceed by rewriting $H(z)$ as

$$H_n(z) = \sin\left(\frac{(2n-1)\pi z}{Z}\right), n = 1, 2, 3, \dots \quad (28)$$

with $\nu = \frac{(2n-1)\pi}{Z}$.

Multiplying by r , Equation (26) can be written as

$$r^2 R'' + rR' + r^2 \mu^2 R = 0.$$

This is a Bessel equation of the first kind of order zero and the general solution is a

linear combination of Bessel functions of the first and second kind,

$$R(r) = c_1 J_0(\mu r) + c_2 N_0(\mu r). \quad (29)$$

Since we wish to have $u(r, z, t)$ bounded at $r = 0$ and $N_0(\mu r)$ is not well behaved at $r = 0$, we set $c_2 = 0$. Up to a constant, Equation (29) becomes

$$R(r) = J_0(\mu r). \quad (30)$$

The boundary condition $R(a) = 0$ gives $J_0(\mu a) = 0$ and thus $\mu_m = \frac{j_{0m}}{a}$, for $m = 1, 2, 3, \dots$. Here j_{0m} is the m^{th} root of the zeroth-order Bessel function above. ($J_0(j_{0m}) = 0$.) This suggests that

$$R_m(r) = J_0\left(\frac{r}{a} j_{0m}\right), m = 1, 2, 3, \dots \quad (31)$$

Thus, we get the general solution

$$u(r, z, t) = \sum_{n=1}^{\infty} \sum_{m=1}^{\infty} A_{nm} \sin\left(\frac{(2n-1)\pi z}{Z}\right) J_0\left(\frac{r}{a} j_{0m}\right) e^{-\lambda_{nm} D t} \quad (32)$$

with $\lambda_{nm} = \left(\left(\frac{(2n-1)\pi}{Z}\right)^2 + \left(\frac{j_{0m}}{a}\right)^2\right)$, for $n, m = 1, 2, 3, \dots$

Using the initial condition to find the A_{nm} 's, we have

$$T_i - T_b = \sum_{n=1}^{\infty} \sum_{m=1}^{\infty} A_{nm} \sin\left[\frac{(2n-1)\pi z}{Z}\right] J_0\left(\frac{r}{a} j_{0m}\right).$$

If we let $b_n(r) = \sum_{m=1}^{\infty} A_{nm} J_0\left(\frac{r}{a} j_{0m}\right)$, we have

$$T_i - T_b = \sum_{n=1}^{\infty} b_n(r) \sin\left(\frac{(2n-1)\pi z}{Z}\right).$$

As seen previously, this is a Fourier sine series and the Fourier coefficients are given

by

$$\begin{aligned}
b_n(r) &= \frac{2}{Z} \int_0^Z (T_i - T_b) \sin\left(\frac{(2n-1)\pi z}{Z}\right) dz \\
&= \frac{2(T_i - T_b)}{Z} \left(-\frac{Z}{(2n-1)\pi} \cos\left(\frac{(2n-1)\pi z}{Z}\right) \right)_0^Z \\
&= \frac{4(T_i - T_b)}{(2n-1)\pi}.
\end{aligned}$$

Then, we have

$$b_n(r) = \frac{4(T_i - T_b)}{(2n-1)\pi} = \sum_{m=1}^{\infty} A_{nm} J_0\left(\frac{r}{a} j_{0m}\right).$$

As before, we need the orthogonality of Bessel functions for $\mu_m = \frac{j_{0m}}{a}$. We have [5]

$$\int_0^a J_0(\mu_m r) J_0(\mu_k r) r dr = \begin{cases} 0, & m \neq k, \\ \frac{a^2}{2} J_1^2(j_{0m}), & m = k. \end{cases}$$

This yields for $b_n(r)$

$$\frac{4(T_i - T_b)}{(2n-1)\pi} = \sum_{m=1}^{\infty} A_{nm} J_0\left(\frac{r}{a} j_{0m}\right).$$

Integrating,

$$\int_0^a \frac{4(T_i - T_b)}{(2n-1)\pi} J_0(\mu_k r) r dr = \int_0^a \sum_{m=1}^{\infty} A_{nm} J_0(\mu_m r) J_0(\mu_k r) r dr.$$

Using $\int_0^a J_0(\mu_m r) J_0(\mu_k r) r dr = \frac{a^2}{2} J_1^2(j_{0m}) \delta_{nm}$, we have

$$\frac{4(T_i - T_b)}{(2n-1)\pi} \int_0^a J_0(\mu_k r) r dr = A_{nm} \left(\frac{a^2}{2} J_1^2(j_{0m}) \right). \quad (33)$$

In order to find $\int_0^a J_0(\mu_k r) r dr$, we let $y = \mu_k r$ and get

$$\int_0^a J_0(\mu_k r) r dr = \int_0^{\mu_k a} J_0(y) \frac{y}{\mu_k} \frac{dy}{\mu_k}$$

$$\begin{aligned}
&= \frac{1}{\mu_k^2} \int_0^{\mu_k a} J_0(y) y dy \\
&= \frac{1}{\mu_k^2} \int_0^{\mu_k a} \frac{d}{dy} (y J_1(y)) dy \tag{34}
\end{aligned}$$

$$= \frac{1}{\mu_k^2} (\mu_k a) J_1(\mu_k a) = \frac{a^2}{j_{0k}} J_1(j_{0k}). \tag{35}$$

Here, in (34), we have made use of the identity $\frac{d}{dx} (x J_1(x)) = J_0(x)$ [5]. Substituting (35) into Equation (33) we have

$$\frac{4(T_i - T_b)}{(2n - 1) \pi} \left(\frac{a^2}{j_{0m}} J_1(j_{0m}) \right) = A_{nm} \left(\frac{a^2}{2} J_1^2(j_{0m}) \right).$$

Solving for A_{nm} , we find

$$A_{nm} = \frac{8(T_i - T_b)}{(2n - 1) \pi} \frac{1}{j_{0m} J_1(j_{0m})}.$$

Substituting A_{nm} into our original expression for $u(r, z, t)$, Equation (32) gives

$$u(r, z, t) = \frac{8(T_i - T_b)}{\pi} \sum_{n=1}^{\infty} \sum_{m=1}^{\infty} \frac{\sin\left(\frac{(2n-1)\pi z}{Z}\right)}{(2n - 1)} \frac{J_0\left(\frac{r}{a} j_{0m}\right) e^{\lambda_{nm} D t}}{j_{0m} J_1(j_{0m})}.$$

Therefore, $T(r, z, t)$ can be found as

$$T(r, z, t) = T_b + \frac{8(T_i - T_b)}{\pi} \sum_{n=1}^{\infty} \sum_{m=1}^{\infty} \frac{\sin\left(\frac{(2n-1)\pi z}{Z}\right)}{(2n - 1)} \frac{J_0\left(\frac{r}{a} j_{0m}\right) e^{\lambda_{nm} D t}}{j_{0m} J_1(j_{0m})}.$$

This gives the general solution for the three-dimensional heat equation in cylindrical coordinates with constant diffusivity. Similar to the solutions shown in Figure 1 of the previous section, Figure 2 shows various temperature progressions throughout a standard 9" round cake pan.

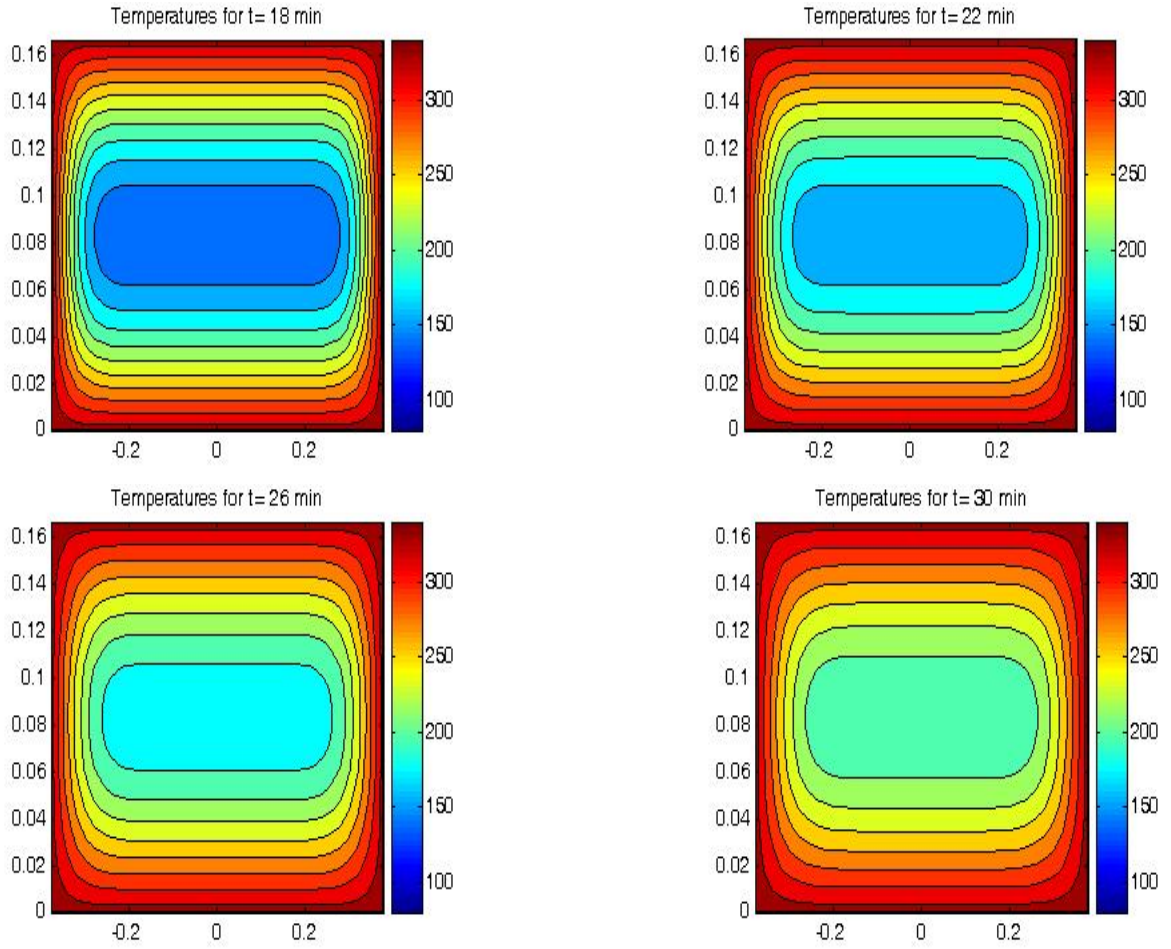


Figure 2: Temperature development throughout a standard 9" cake shown as vertical slices through the center. Radius horizontal and height vertical are given in feet.

3 CONSTANT D VALUES

Now that we have reviewed some exact series solutions, we can use the data collected by Dr. Olszewski to explore the rates for which heat diffuses throughout each cake. Since the data was found using cylindrical cakes [2], we will hereafter refer to the three-dimensional heat equation in cylindrical coordinates. In this section we will determine constant values of D using real baking times.

Seven different gènoise cakes were baked [2] in four different diameter pans filled with batter to various heights, for which the ingredients are listed in Table 1. This recipe was chosen for simplification purposes, as there is minimal rise of the batter throughout the baking process [2].

	Traditional measure	Dry measure (g)
Eggs	6 large	298
Sugar	3/4 cup	176
Vanilla extract	1/2 tsp	2
All purpose flour	1 cup	144
Butter	3/4 stick	114

Table 1: Ingredients for the gènoise recipe given in traditional and metric dry measures

The temperature of each batter was recorded every minute at the center of the cake until reaching 203°F, the desired center temperature determined for a done cake [2]. The cake sizes and their times taken to bake are given in Table 2. The dimensions are given in inches, with radii rounded to the nearest tenth of an inch, and the time is given in minutes. The height designates the depth of batter in the pan when initially placed in the oven.

In order to find the diffusion constants needed to produce the desired center temperature for the given baking times cake dimensions, we used MATLAB[®] to program the series solutions found in Section 2.2. *Diffusion.m*, found in Appendix A, takes the given data and evaluates the final temperature at the center of the

Diameter (in.)	Radius (in.)	Height (in.)	Time (min.)
13.0	6.5	1.6	35
9.9	5.0	1.8	41
9.9	5.0	1.6	20
8.0	4.0	1.0	17
4.1	2.1	4.0	26
4.1	2.1	2.0	20
4.1	2.1	1.8	19

Table 2: Cake sizes and their baking times.

cake. Given the correct value of D , the desired final temperature of 203°F will be reached. We must also evaluate the first several zeros, j_{0m} , in order to complete the solutions. We have done so using *besselj.m* [3], found in Appendix B, in conjunction with *Diffusion.m*. An example of the plot that is produced is shown in Figure 3. The correct value for D is found when $u(r, z, t) = 203^\circ\text{F}$.

Our initial attempted D values were based on those found by Dr. Olszewski in his non-constant diffusion case [2]. These produced well above the desired final temperature, which led to the need of further examination of his values. The difference found was in part due to the fact that his diffusion rates are given in in^2/min compared to our chosen ft^2/min . Also, only the first term of the series solutions were used in calculating his D values. After a series of trial and error runs of slowly refining smaller values of D , the diffusion rates we found to satisfy the given dimensions, baking time and center temperature, as are listed in Table 3. Converting our diffusion rates into in^2/min found that the reduction in terms used produced as much as six times the diffusion rate needed to reach the desired center temperature of 203°F.

Since cakes of relatively the same radius were hypothesized to have similar diffusivity [2], the trial process was initially minimized. However, as can be seen in Table 3, Cakes 4 and 7 are of the same radius but their D values are more similar

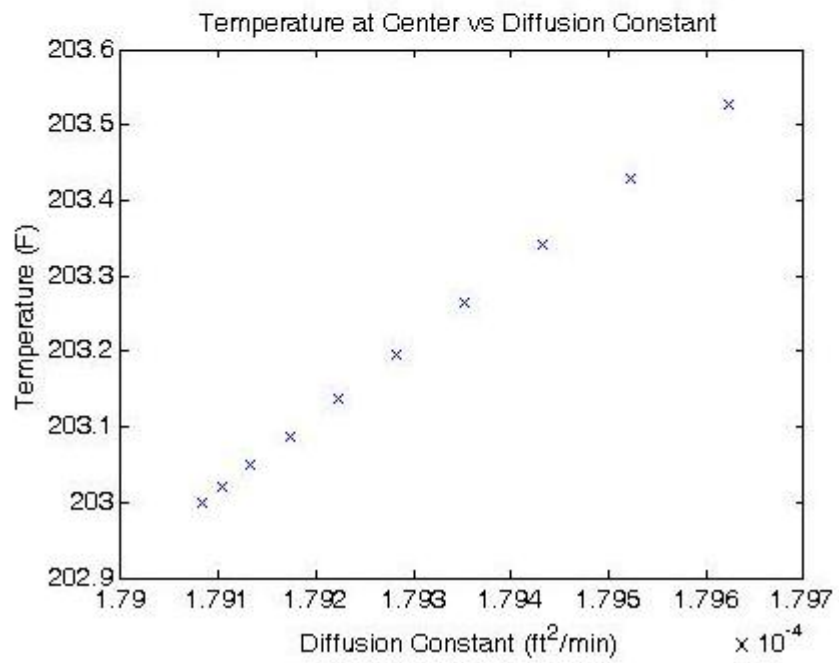
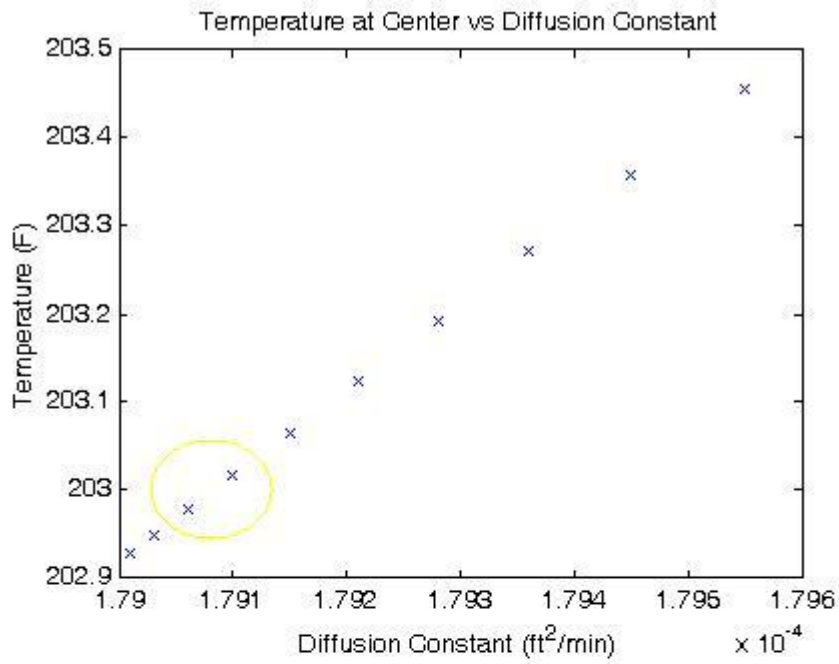


Figure 3: The first graph shows an initial trial of diffusion.m using $D = 17.9 \times 10^{-5} \text{ ft}^2/\text{min}$. Refining our results led to the final solution of $D = 17.9073 \times 10^{-5} \text{ ft}^2/\text{min}$.

	Height (in.)	Radius (in.)	Time (min)	D (ft^2/min)
1	4.0	2.1	26	17.91×10^{-5}
2	2.0	2.1	20	11.08×10^{-5}
3	1.8	2.1	19	9.81×10^{-5}
4	1.8	5.0	41	4.72×10^{-5}
5	1.6	6.5	35	4.37×10^{-5}
6	1.0	4.0	17	3.51×10^{-5}
7	1.0	5.0	20	2.99×10^{-5}

Table 3: Diffusion constants determined from given dimensions and known baking time to reach 203°F.

to those of Cakes 5 and 6, respectively. Noting that the heights of Cakes 4, 5 and 6, 7 are also closer in value lead to the reordering of Table 3 by Height rather than by Diameter as in Table 2.

In general, the diffusivity is shown to be largest in cakes with smaller radii as stated in by Dr. Olszewski, except for when the height is also less, as with Cakes 5 and 6. Since moisture evaporates from both the top and sides of the cake, the drier batter that is left behind causes a decrease in heat diffusion [1][2]. This brings to question whether or not the decrease or increase in diffusion is more greatly affected by the change in radius or height. The data in Table 3 would suggest that the height of the cake has the strongest influence on the heat diffusivity of the batter. Yet seeing how the D values of Cakes 6 and 7 were altered by the radius would suggest otherwise, or at least not in all cases.

Although the height decreases down the table, the radii vary in comparison from one to the next. This led us to the explore the effect on the heat diffusion of the cakes due to the ratio of height to radius. The results shown in Table 4 show that the ratio of the height to radius has a direct correlation to the rate of diffusion; as the ratio decreases, so does the diffusion rate. Similarly, an inverse relationship is seen when comparing the ratio of radius to height. (Note: The ratios of Cakes 5 and 6 do not follow the increasing pattern but when rounded are equal.)

	$D \text{ ft}^2/\text{min}$	H/R	R/H
1	17.91×10^{-5}	1.9048	0.525
2	11.08×10^{-5}	0.9524	1.05
3	9.81×10^{-5}	0.8571	1.1667
4	4.72×10^{-5}	0.36	2.7778
5	4.37×10^{-5}	0.2462	4.0625
6	3.51×10^{-5}	0.25	4.0
7	2.99×10^{-5}	0.202	5.0

Table 4: Diffusion constants compared to the ratios of radius and height values.

Figure(4) shows the dependence of the diffusion rate on $x = H/R$ is approximately linear.

$$D = (8.765 \times 10^{-5})x + 1.797 \times 10^{-5}. \quad (36)$$

This linear regression gives a correlation coefficient of $r \approx .994$.

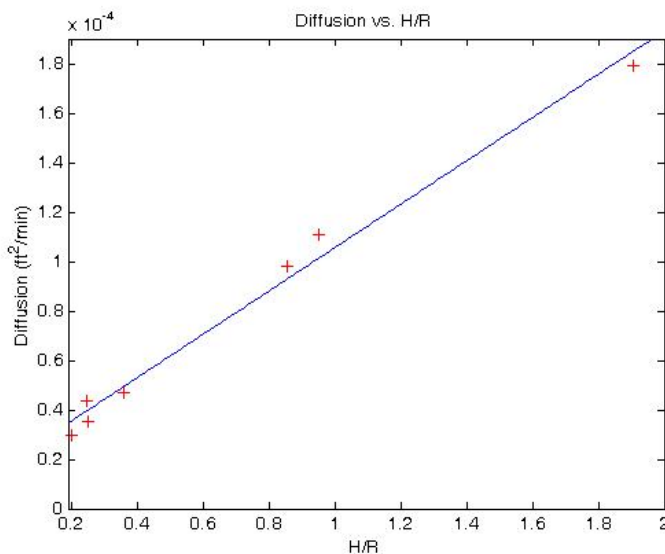


Figure 4: A strong positive linear approximation of $D \text{ ft}^2/\text{min}$, given the ratio of H/R.

Likewise, it was found that the comparison of $x = R/H$ to the diffusion rate followed a logarithmic approximation, with a correlation coefficient of $r \approx -.977$.

Figure 5 shows this relationship approximated by

$$D = 1.220 \times 10^{-4} - (6.227 \times 10^{-5}) \ln(x). \quad (37)$$

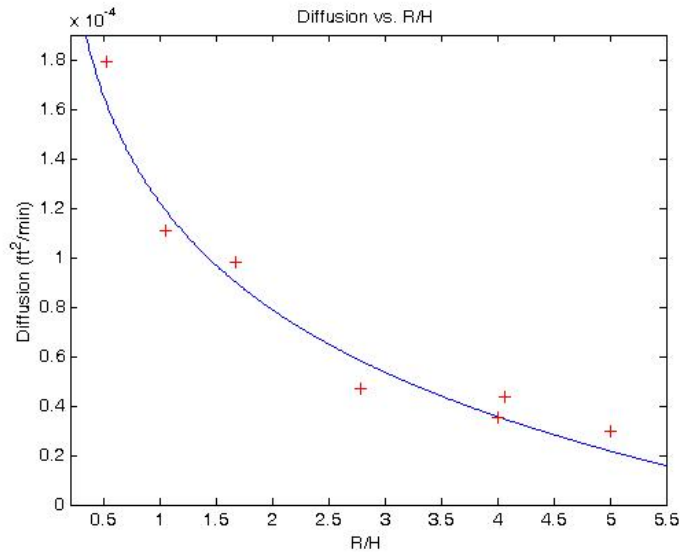


Figure 5: A logarithmic approximation of D ft²/min, given the ratio of R/H.

From Figures 4 and 5, and Table 4 we can conclude that for similar cakes, (those with the same height and varying radii, and vice versa) a decrease or increase in the varying parameter causes a decrease or increase in volume, respectively. This could lead one to think diffusion is then affected by the volume of batter and not simply by the ratio of height to radius as is concluded in Figure 5. However, upon a closer look, one can see that for cakes of the same radius and varying height (as in Cakes 1-3) diffusion decreases as the height decreases. Yet for Cakes such as 3 and 4, a decrease in radius with the same height causes an increase in diffusion. Therefore, we can conclude that volume does not affect the rate, which one could have also seen by noting the square of the radii of Cakes 5-7 and the product of their respective heights to be greatly out of order.

However, keeping the term volume loosely in mind, for our given data, a greater H/R ratio corresponds to a more compact, or “circularly square” cake. As this ratio decreases, the cake flattens and elongates, and the diffusion rate decreases. Since no data was collected for a cake of greater height than diameter, we can merely use Equation (37) to estimate that an increase in this ratio, corresponding to a tall cake, would also increase the diffusion rate. However, we can not state this for certain due to the possibility that these rates could possibly plateau for proportions approximately equal to one and then decrease in the same fashion as the cakes increase in height and decrease in radius.

A similar synopsis can be shown for larger R/H ratios. A greater ratio corresponds to the elongated cake mentioned previously, and does in fact correspond to the lessened diffusion, as seen in Table 4. This re-instates that the rate of diffusion changes with the proportion of dimensions, or geometry of the cake, which brings up the question of a diffusion change in correspondence with the change in surface area. For example, the described “square” cake has a greater lateral surface area than that of the elongated cakes. Table 5 shows the ratios between the lateral and radial surface areas, denoted as $SA_h = 2\pi RH$ and $SA_r = \pi R^2$ respectively, and the diffusion rates of each cake.

	$D \text{ ft}^2/\text{min}$	SA_h/SA_r	SA_r/SA_h
1	17.91×10^{-5}	3.8095	0.2625
2	11.08×10^{-5}	1.9048	0.525
3	9.81×10^{-5}	1.7143	0.583
4	4.72×10^{-5}	0.72	1.3889
5	4.37×10^{-5}	0.4923	2.0313
6	3.51×10^{-5}	0.5	2.0
7	2.99×10^{-5}	0.4	2.5

Table 5: Diffusion constants compared to the ratios of the surface areas SA_h and SA_r .

From Table 5 we can see results similar to those found in Table 4, which should

be expected as the ratios of each surface area reduces to $\frac{2H}{R}$ and $\frac{R}{2H}$, respectively. We again find a stronger linear correlation ($r \approx .994$) between the lateral surface area ratio, SA_h/SA_r , and the diffusion values, compared to the logarithmic correlation ($r \approx -.977$) between the radial ratio SA_r/SA_h and diffusion. Figure 6 shows the linear correlation of D as approximately

$$D = (4.382 \times 10^{-5})x + 1.797 \times 10^{-5},$$

as well as the logarithmic correlation as approximately

$$D = 7.880 \times 10^{-5} - (6.226 \times 10^{-5}) \ln(x).$$

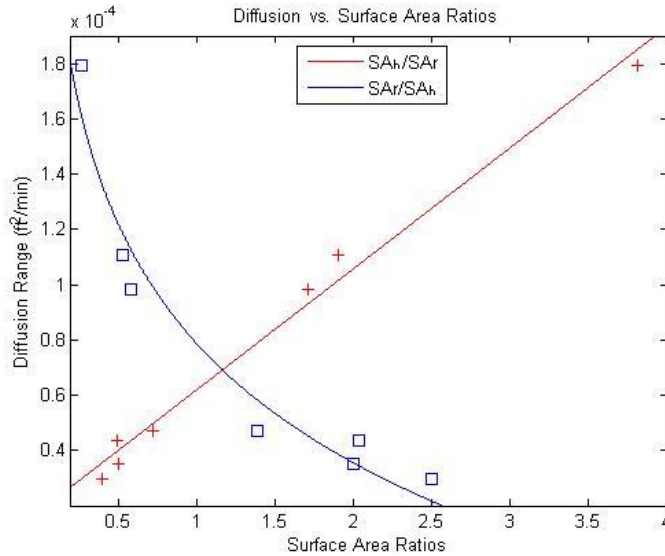


Figure 6: Approximations of D (ft^2/sec), given the ratios of SA_z/SA_r and SA_r/SA_z .

Thus, we once again show that taller cakes have greater diffusion throughout the baking process. These findings can also be used to discuss, in general, how even though cookies and other pastries have substantially less batter to be baked, they take a relatively long time to do so [2]. The lesser ratio of lateral surface area causes

a reduced rate of diffusion, which in turn causes a slower heating process. However, this brings us to some of the assumptions which have been made throughout this process which we must include in order to fully summarize the results found thus far. Although cookies have a substantial baking time per their unit volume, they also contain a higher liquid content. Our current results are based simplistically on the idea that diffusion is affected by spatial positioning of the batter and do not take into account moisture and the process of vaporization that is also occurring simultaneously. In the following chapters, we will discuss how this process also affects the rate of diffusion, invalidating our current constant diffusion premise.

4 FINITE DIFFERENCE SCHEME

In the previous chapters we have discussed the heat equation assuming that the heat diffusivity remains constant throughout the baking/heating process. This assumption simplifies the heat equation to where it can be solved by hand using the found series solutions. However, in this and the following chapter we will explore the more realistic cases in which diffusion is not assumed constant.

We recall from the derivation of our modeled heat equation as

$$\frac{\partial u}{\partial t} = \nabla \cdot (D \nabla u), \quad (38)$$

for $D = \frac{K_0(r,z)}{c\rho}$. Then

$$\begin{aligned} \frac{\partial u}{\partial t} &= \frac{1}{r} \frac{\partial}{\partial r} \left(r D \frac{\partial u}{\partial r} \right) + \frac{\partial}{\partial z} \left(D \frac{\partial u}{\partial z} \right) \\ &= \frac{1}{r} \left(D \frac{\partial u}{\partial r} + r \frac{\partial D}{\partial r} \frac{\partial u}{\partial r} + r D \frac{\partial^2 u}{\partial r^2} \right) + \frac{\partial D}{\partial z} \frac{\partial u}{\partial z} + D \frac{\partial^2 u}{\partial z^2}. \end{aligned} \quad (39)$$

To solve this equation, we use a finite difference method. We have chosen to use a center difference scheme [4] for the spatial derivatives on the right and the typical forward difference scheme for the time derivative. One could just as easily use strictly one method or the other.

We can approximate, for example, in the positive radial direction, $u(r + \Delta r)$, as

$$u|_{r+} \approx u + \Delta r u' + \frac{\Delta r^2}{2} u'' + \dots,$$

where u , u' , and u'' are evaluated at r and the primes denote the derivatives of u with respect to r . Likewise, the in the $r - \Delta r$ direction,

$$u|_{r-} \approx u - \Delta r u' + \frac{\Delta r^2}{2} u'' + \dots.$$

Thus we can arrange a combination of the two to approximate the first and second derivatives as

$$\begin{aligned}\frac{\partial u}{\partial r} &= \frac{u|_{r+} - u|_{r-}}{2\Delta r} \\ \frac{\partial^2 u}{\partial r^2} &= \frac{u|_{r+} - 2u + u|_{r-}}{\Delta r^2}.\end{aligned}$$

Applying the same technique to D and in the z direction, we can approximate the right hand side of Equation (38) by

$$\begin{aligned}& \frac{1}{r} \left(D \frac{u_{i+1}^n - u_{i-1}^n}{2\Delta r} + r \frac{D_{i+1} - D_{i-1}}{2\Delta r} \frac{u_{i+1}^n - u_{i-1}^n}{2\Delta r} + r D \frac{u_{i+1}^n - 2u_{i,j}^n + u_{i-1}^n}{\Delta r^2} \right) \\ & + \frac{D_{j+1} - D_{j-1}}{2\Delta z} \frac{u_{j+1}^n - u_{j-1}^n}{2\Delta z} + D \frac{u_{j+1}^n - 2u_{i,j}^n + u_{j-1}^n}{\Delta z^2}.\end{aligned}\quad (40)$$

Here, the superscript notation, u^n , denotes the current time step. To save space, the subscript notation is abbreviated to only include one of the two spatial directions at a time. Thus $u_i^n = u_{i,0}^n$ and $u_j^n = u_{0,j}^n$, as well as in the $i \pm 1$ and $j \pm 1$ terms, respectively. Similarly, $D_i = D_{i,0}$ and $D_j = D_{0,j}$. An expanded version can be seen in Appendix C.

Similarly, the time derivative on the left hand side of Equation (38) can be approximated to be

$$\frac{u_{i,j}^{n+1} - u_{i,j}^n}{\Delta t},$$

where $u_{i,j}^{n+1}$ denotes the positive (forward) time given the current values for r and z .

Thus Equation (37) becomes

$$\begin{aligned}\frac{u_{i,j}^{n+1} - u_{i,j}^n}{\Delta t} &= \frac{1}{r} \left(D \frac{u_{i+1}^n - u_{i-1}^n}{2\Delta r} + r \frac{D_{i+1} - D_{i-1}}{2\Delta r} \frac{u_{i+1}^n - u_{i-1}^n}{2\Delta r} + r D \frac{u_{i+1}^n - 2u_{i,j}^n + u_{i-1}^n}{\Delta r^2} \right) \\ & + \frac{D_{j+1} - D_{j-1}}{2\Delta z} \frac{u_{j+1}^n - u_{j-1}^n}{2\Delta z} + D \frac{u_{j+1}^n - 2u_{i,j}^n + u_{j-1}^n}{\Delta z^2}.\end{aligned}$$

To simplify, we let D_{ur} represent the r derivatives and D_{uz} the z , which condenses to

$$u_{i,j}^{n+1} = u_{i,j}^n + \Delta t \left[\frac{1}{r} D_{ur} + D_{uz} \right]. \quad (41)$$

We will look at D_{ur} first. From (40) we have

$$\begin{aligned} D_{ur} &= D \frac{u_{i+1}^n - u_{i-1}^n}{2\Delta r} + r \frac{D_{i+1} - D_{i-1}}{2\Delta r} \frac{u_{i+1}^n - u_{i-1}^n}{2\Delta r} + r D \frac{u_{i+1}^n - 2u_{i,j}^n + u_{i-1}^n}{\Delta r^2} \\ &= \frac{2(\Delta r) D u_{i+1}^n - 2(\Delta r) D u_{i-1}^n + r D_{i+1} u_{i+1}^n - r D_{i-1} u_{i-1}^n - r D_{i-1} u_{i+1}^n + r D_{i+1} u_{i-1}^n}{4\Delta r^2} \\ &\quad + \frac{4r D u_{i+1}^n - 8r D u_{i,j}^n + 4r D u_{i-1}^n}{4\Delta r^4} \end{aligned}$$

Then, combining like temperature terms, u^n , we can rewrite D_{ur} as

$$\begin{aligned} D_{ur} &= u_{i-1}^n \frac{(D_{i-1} r_i + 2D_{i,j}(r_{i-1} + r_i) - D_{i+1} r_i)}{4\Delta r^2} - 2u_{i,j}^n \frac{D_{i,j} r_i}{\Delta r^2} \\ &\quad - u_{i+1}^n \frac{(D_{j-1} r_i - 2D_{i,j}(r_i + r_{i+1}) - D_{j+1} r_i)}{4\Delta r^2}. \end{aligned}$$

Here, the $r_{i\pm 1}$ are used to further simplify our combined $u_{n\pm 1}$'s. For example, in the u_{i-1} term we have $4Dr - 2D(\Delta r)$ which can be rewritten as $2D(2r - \Delta r) = 2Dr_{i-1} + 2Dr_i$. Following the same method for D_{uz} , we have

$$D_{uz} = u_{j-1}^n \frac{D_{j-1} + 4D_{i,j} - D_{j+1}}{4\Delta z^2} - 2u_{i,j}^n \frac{D_{i,j}}{\Delta z^2} + u_{j+1}^n \frac{D_{j-1} + 4D_{i,j} + D_{i,j}}{4\Delta z^2}.$$

Thus, the solution for Equation (38) is written as

$$u_{i,j}^{n+1} = u_{i,j}^n + \Delta t \left[\frac{1}{r} D_{ur} + D_{uz} \right],$$

for

$$D_{ur} = u_{i-1}^n \frac{(D_{i-1} r_i + 2D_{i,j}(r_{i-1} + r_i) - D_{i+1} r_i)}{4\Delta r^2} - 2u_{i,j}^n \frac{D_{i,j} r_i}{\Delta r^2}$$

$$-u_{i+1}^n \frac{(D_{j-1}r_i - 2D_{i,j}(r_i + r_{i+1}) - D_{j+1}r_i)}{4\Delta r^2},$$

and

$$D_{uz} = u_{j-1}^n \frac{D_{j-1} + 4D_{i,j} - D_{j+1}}{4\Delta z^2} - 2u_{i,j}^n \frac{D_{i,j}}{\Delta z^2} + u_{j+1}^n \frac{D_{j-1} + 4D_{i,j} + D_{i,j}}{4\Delta z^2}.$$

At this point we have not thoroughly investigated the truncation error of this scheme.

We will leave this for future analysis.

We have used a combination of *heatcylfd.m* and *heatcylFD.m*, found in Appendix C, to implement this scheme. Given the cake dimensions and baking times we can determine the types of nonconstant diffusivities which will yield the desired 203°F in the specified amount of time. We have chosen to use Cake 1 (height 4 inches and radius 2.1 inches) to numerically model this scheme. These findings will be discussed in the following chapter.

5 NUMERICAL SOLUTIONS

Previously, we have assumed that heat diffuses at a constant rate throughout the baking process. However, since cakes begin as moist batter and develop into drier cake consistencies, we must take into account the fact that different materials transfer heat at different rates. Dr. Olszewski does this by assuming that moisture flows through the batter from bottom to top (or evaporates from top to bottom), causing the top half of the cake to be the drier consistency than bottom half [2]. He then adapts his original process to incorporate two values of D to correspond to these two halves of different consistency determined by a boundary $z = \text{constant}$, independent of r . To do so he assumes D to be dependent upon time.

We would like, however, to explore the idea that the two consistencies do not separate the cake in half, but instead form in symmetric "rings" as implied from Figures 1 and 2. Since the cake pan would likely have the same effect on the surrounding batter as the oven temperature does on the exposed top, we feel the baking process should be fairly consistent and symmetric throughout. Also, as these areas heat and decrease in temperature difference from their surroundings, their diffusivity decreases and thus is dependent primarily upon position and temperature. How much so and to what degree these changes occur would then depend upon the amount of time exposed to the higher surrounding temperatures. Thus, we would like to find a diffusion equation to model these aspects of the baking process. The derivation of the heat equation from Chapter 1 allows us to do just this. We have chosen to model D for three different cases: 1) Having two constant diffusion values correspond to the two states of batter, thus changing dependent upon the temperature; 2) Softening the gap between these values via a piecewise-linear function; and 3) Further refining the change with a smooth non-linear curve.

5.1 Piecewise Constant D Case

We begin by assigning D_1 as the initial diffusivity of the moist batter and D_2 as that of the drier cake. We know that as water in the batter reaches 212°F , evaporation occurs leaving behind the drier cake consistency. Thus, by denoting T_1 as the initial temperature of the batter (80°F) and T_2 as the boiling temperature (212°F), for our piecewise constant D case we let D_1 represent the diffusivity as portions of the batter heat to this boiling point, for $T_1 \leq T < T_2$,

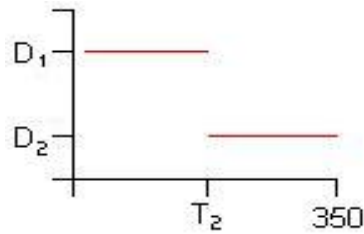


Figure 7: Heat diffusion change between two constant rates given the current temperature.

and D_2 by the diffusion throughout the higher temperature, $T_2 \leq T \leq 350^\circ$, portions batter for the duration of the baking process. Since the temperature difference between the batter and oven is greatest initially and then decreases as the batter heats, $D_1 > D_2$.

Our next step is to determine the actual values of D_1 and D_2 for which the diffusion rates change. Recalling from Chapter 3, the original constant D was found to be $17.9073 \times 10^{-5} \text{ ft}^2/\text{min}$ for our specified cake. Supposing this rate to be an average throughout, we followed a similar trial and error process as in the single constant case. Several ranges of D values were found to produce the desired 203°F center temperature for the baking time of 26 minutes. A sample of these ranges is shown in Table 6.

As we vary the diffusion rates, we notice an inverse correlation between D_1 and D_2 which suggests some validity of maintaining an overall average rate of diffusion

D_1 ft ² /min	D_2 ft ² /min	T (°F)
$18.5 \times (10)^{-5}$	$16.5 \times (10)^{-5}$	203.1
$19.0 \times (10)^{-5}$	$16.0 \times (10)^{-5}$	202.8
$20.0 \times (10)^{-5}$	$15.2 \times (10)^{-5}$	203.1
$20.5 \times (10)^{-5}$	$14.7 \times (10)^{-5}$	202.8
$21.0 \times (10)^{-5}$	$14.5 \times (10)^{-5}$	203.5
$21.5 \times (10)^{-5}$	$14.0 \times (10)^{-5}$	203.2
$24.0 \times (10)^{-5}$	$12.2 \times (10)^{-5}$	202.8

Table 6: Center temperatures given a variety of D ranges between two constant rates.

throughout the baking process as mentioned above. Since the center temperature differences between these values is negligible, any could be used to model our two constant D case. However, we would like to analyze the baking implications of using any arbitrary range of diffusion rates.

The two larger range values shown in the last entry of Table 6 would seem to imply a steady high, unchanging D_1 rate of heating for the first half of the process and then dropping to the low, unchanging rate of D_2 for the remaining baking time. To one who is familiar with baking, or cooking in general, this scenario would seem to yield a possible over-drying, or burning, of the cake closest to the pan and top surface, leaving it less than desirable. Conversely, choosing a shorter range would seem to yield results similar to the single constant diffusion rate for which we are trying to redefine. Thus, we have chosen to use the following two constant D model:

$$D = \begin{cases} D_1 = 20.0 \times (10)^{-5} & \text{for } T_1 \leq T_2, \\ D_2 = 15.2 \times (10)^{-5} & \text{for } T_2 \leq T < 350^\circ\text{F}. \end{cases}$$

Having a reasonable difference between diffusion rates, we feel this scenario best represents the gradual baking environment needed to obtain the final, moist cake consistency which is most commonly sought after.

Figure 8 are thermal layers throughout the cake, taken as vertical slices through

the center of the cake for the indicated times by implementing the piecewise constant D function into the cylindrical cake solutions in *heatcylfd.m* and *heatcylFD.m*, found in Appendix C.

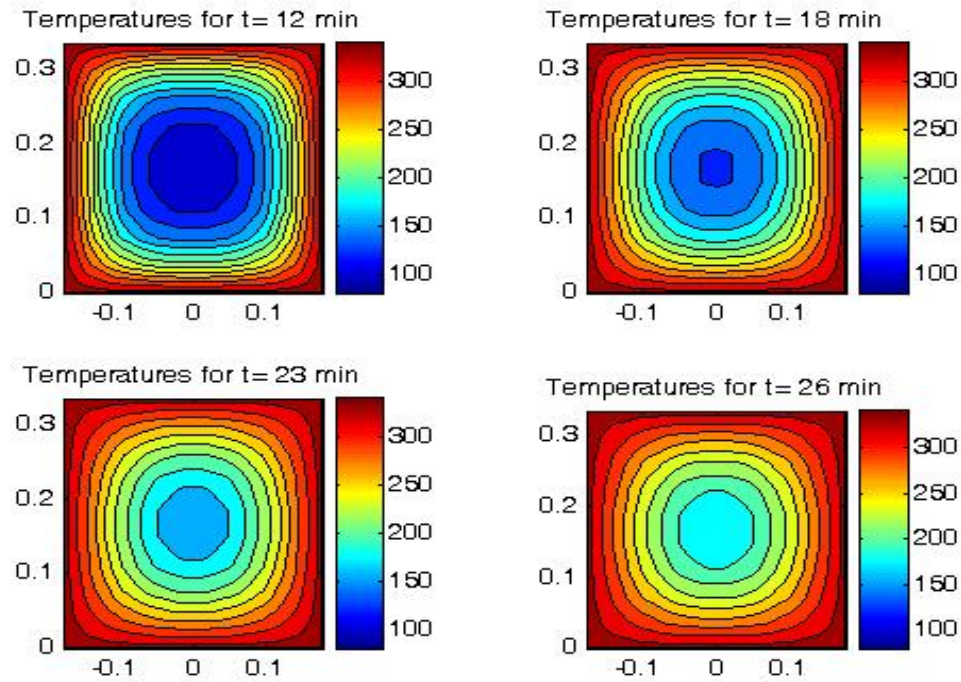


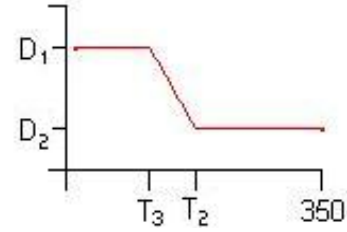
Figure 8: Center temperatures given piecewise constant diffusivity. Height vertical and radius horizontal are shown in feet.

Each figure represents a “slice” through the center of the cake, $r = 0$, for the specified times and reveals the positional and temperature symmetry as mentioned above. The lower right image shows the center temperature at 26 minutes to be approximately 203°F. Although this is more realistic than the single constant D case, the immediate change from one constant diffusion rate to another is still unreasonable, since both the heating and baking processes are gradual. Thus in the following sections we would like to continue to redefine our diffusion process.

5.2 Linear Approximation of D Values

Having noted the idea of a gradual change in heat throughout the baking process, we would like to now examine the possible rates for which this change between consistencies and their diffusivities occur. We again suppose D_2 to be the rate of diffusion through the drier cake portions for temperatures greater than 212°F and let D_1 to be that of the moist batter. We now assume that the diffusivity decreases linearly from D_1 to D_2 for $T \leq 212^\circ\text{F}$. The starting point of this decrease is assumed to be $T_3 = T_2 - c$, for $c \geq 0$ an arbitrary temperature difference from T_2 . The corresponding diffusion parameter D could thus be represented by the following piecewise function:

$$D = \begin{cases} D_1 & \text{for } T_1 \leq T < T_3, \\ \beta(T - T_4) + b & \text{for } T_3 \leq T < T_2, \\ D_2 & \text{for } T_2 \leq T < 350^\circ, \end{cases}$$



for $\beta = \frac{D_2 - D_1}{T_2 - T_3}$, b the midpoint of D_1 and D_2 , and T_4 the midpoint of T_3 and T_2 .

Therefore,

$$\beta(T - T_4) + b = \frac{D_2 - D_1}{T_2 - T_3} \left[T - \frac{T_3 + T_2}{2} \right] + \frac{D_1 + D_2}{2}.$$

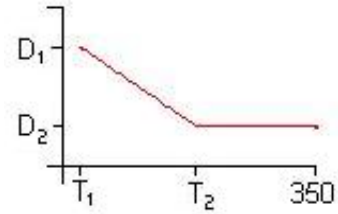
Technically speaking, this decrease should begin as soon as the cake is placed in the oven and begins to heat. However, we will explore for which values of c , if any, yield our desired 203°F center temperature.

Given the current range of diffusion rates, $D_2 = 15.2 \times 10^{-5} \text{ ft}^2/\text{min}$ to $D_1 = 20.0 \times 10^{-5} \text{ ft}^2/\text{min}$, from Section 5.1, one should expect any value other than $c = 0^\circ\text{F}$ to decrease the amount of initial heat diffusion and therefore cause a decrease in the final temperature. Using the same code (found in Appendix C) as in the previous section, by increasing c in increments of 25°F , we recorded the

center temperature attained at the baking time of 26 minutes. As was expected, the final center temperature decreased by approximately 2°F on average, leaving an unsatisfactory value of c , given our current range of diffusion rates. We only obtain similar temperature results when $c \approx 0$.

We have chosen to examine the original idea that the diffusivity is immediately altered as the batter is placed in the oven and begins to heat, causing a decrease in the rate of diffusion. We must then determine a new range of diffusion rates which will result in the desired center temperature. We choose $c = 132^\circ\text{F}$, which corresponds to $T_3 = T_1$. Our updated diffusion equation then becomes:

$$D = \begin{cases} \beta(T - T_4) + b & \text{for } T_1 \leq T < T_2, \\ D_2 & \text{for } T_2 \leq T < 350^\circ, \end{cases}$$



where

$$\beta(T - T_4) + b = \frac{D_2 - D_1}{T_2 - T_1} \left(T - \frac{T_1 + T_2}{2} \right) + \frac{D_1 + D_2}{2}.$$

We note that the center temperature of the batter changes minimally ($< 1^\circ\text{F}$) until approximately 3 minutes into the baking process. Thus, we could have chosen to let $c = 129^\circ\text{F}$ and adapted the original D respectively. However, the temperature difference at the center between these two cases was found to be $< 1^\circ\text{F}$ so we continue with the $c = 132^\circ\text{F}$ case.

Now we must find a new range of diffusion rates which will yield the desired center temperature in the allotted baking time. Using the same trial and error, and evaluation of realistic D rates, as before,

$$D_1 = 25 \times 10^{-5} \text{ft}^2/\text{min} \quad \text{and} \quad D_2 = 17 \times 10^{-5} \text{ft}^2/\text{min}$$

were found to produce approximately 203°F at 26 minutes as shown in Figure 4.

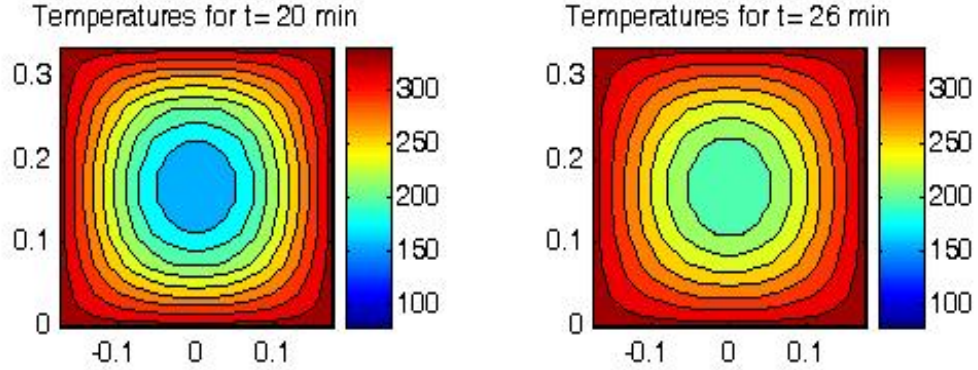


Figure 9: Center temperatures given linear D , for $T_3 = T_1$. Height vertical and radius horizontal in feet.

We again analyze the corresponding baking scenario derived given this range of diffusion rates. As the initial batter at T_1 is exposed to the oven temperature, it begins to heat accordingly which decreases the rate of heat diffusion throughout these heated regions. In our previous model, we hesitated to use larger D_1 values due to the possible over-drying of the outer regions. However, since we are now assuming the rate of D_1 to decrease at a constant rate, the more exposed portions of batter are initially heated quickly but then lessen as the temperature difference decreases, causing reduced heat diffusion. Our previous model did not take into account this heat gain acquired between T_1 and T_2 . Although a decent approximation of the heating process, we feel this new variation

$$D = \begin{cases} \beta(T - T_4) + b & \text{for } T_1 \leq T < T_2, \\ D_2 = 17 \times (10)^{-5} \text{ft}^2/\text{min} & \text{for } T_2 \leq T < 350^\circ. \end{cases}$$

for

$$\begin{cases} \beta = \frac{D_2 - D_1}{T_2 - T_3} & D_1 = 25 \times 10^{-5} \text{ft}^2/\text{min} \\ T_4 = \frac{T_3 + T_2}{2} & b = \frac{D_1 + D_2}{2}, \end{cases}$$

better accommodates the actual heat increase and diffusion decrease associated with the initial portion of the baking process.

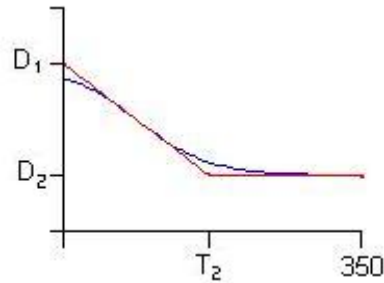
This being said, we also find a flaw in the linear approximation. Although we have now taken into account the initial temperature gain, we fail to note the continuing change even after portions of the batter reach and exceed their boiling point at T_2 . The following section will then show an attempt to refine our diffusion problem once more, and find a suitable function for D that accommodates *all* aspects of the baking process.

5.3 Non-Linear Approximation of D Values

We continue to refine our diffusion model by smoothing out the linear function to incorporate higher temperature diffusion. As mentioned in the previous sections, any diffusion occurring throughout high temperature regions ($> T_2$) remains unchanged through the duration of the baking time. We wish to smooth out our current piecewise continuous approximation. We choose a non-linear hyperbolic tangent function of the form

$$D = a \tanh [\beta(T - T_4)] + b, \text{ for}$$

$$a = \frac{D_1 - D_2}{2}, \quad \beta = \frac{D_2 - D_1}{T_2 - T_3}, \quad b = \frac{T_3 + T_2}{2}.$$



Since our linear function passes through a central point of $(T_4, \frac{D_1 + D_2}{2})$, these coefficients ensure the placement and amplitude of our hyperbolic corresponds to the range and temperature values of the linear function as seen above. We must also make sure that the slope of our new function is the same as the linear model's β at

$T = T_4$. Thus we need

$$D'(T_4) = a\beta \operatorname{sech}^2 [\beta(T - T_4)] = \beta.$$

However, one can see that this yields a slope of $a\beta$, given that $\operatorname{sech}^2 [\beta(T_4 - T_4)] = 1$.

To compensate, we divide β in the function above by a which results in

$$D = a \tanh \left[\frac{\beta}{a}(T - T_4) \right] + b.$$

This current notation corresponds to that of $\alpha = 3$ in *heatD.m* of Appendix C. By using *plotD.m*, found in Appendix D, we can visualize the coordination of our linear and hyperbolic tangent curves in Figure 5 given the temperature and previous range of D values. Here we can see the continuing change in diffusion rates as regions reach and exceed their boiling point at T_2 .

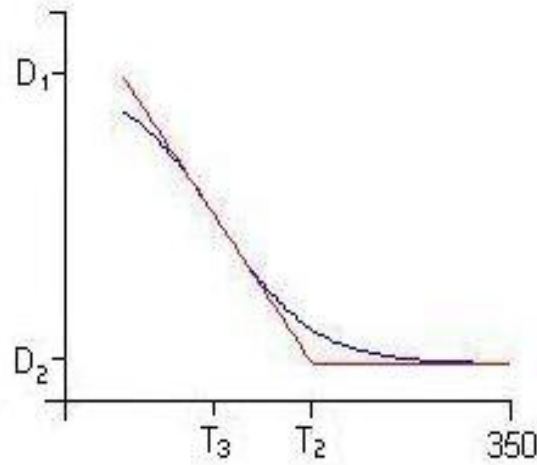


Figure 10: Linear and Hyperbolic Tangent curves given temperature and D values.

Satisfied with our new D approximation, we implemented the curve into the same codes as before found in Appendix C. Also noting the reduced range of D values spanned by our hyperbolic function, it came to no surprise that given the current

values, the center temperature of the cake only reached approximately 190°F. Thus once again manipulating our range of diffusion rates, we found that for

$$D_1 = 23 \times 10^{-5} \text{ft}^2/\text{min} \quad \text{and} \quad D_2 = 16.3 \times 10^{-5} \text{ft}^2/\text{min},$$

we attained a center temperature of approximately 203°F as seen in Figure 6.

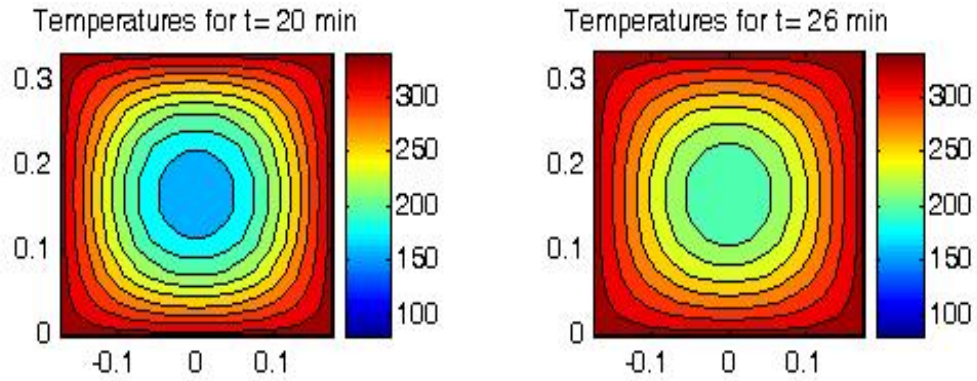


Figure 11: Center temperatures given hyperbolic D . Height vertical and radius horizontal are shown in feet.

We would like to note this range of D values was the smallest possible range for which we could satisfy the 203°F center temperature requirement at the baking time for 26 minutes given the cake dimensions in question. Other, larger ranges produced similar results as in the previous sections, however we once again speculate that a smaller range of diffusion best suites an environment for quality baking standards. Thus we feel the diffusion function

$$D = a \tanh(\beta(T - T_4)) + b,$$

for

$$D_1 = 23 \times 10^{-5} \text{ ft}^2/\text{min} \quad D_2 = 16.3 \times 10^{-5} \text{ ft}^2/\text{min}$$

$$a = \frac{D_1 - D_2}{2}, \quad \beta = \frac{D_2 - D_1}{T_2 - T_3}, \quad b = \frac{T_3 + T_2}{2},$$

is a satisfactory model for our specified cake dimensions. In the next section we will compare each of our approximations to see how much change actually occurs between the varying functions.

5.4 Comparison of Diffusion Models

For the three models highlighted in the previous sections of this chapter, we can compare the temperature differences obtained between each function. Referring to the contour plots at the bottom of *heatFDcyl.m*, each function defined is plotted and labeled as *C1*, *C2*, and *C3* respectively. Each plot is then paired with one of the either remaining and the absolute value of their temperature differences is recorded and shown as a line contour for easier viewing. We have then manually selected various points on these contour rings to illustrate the temperature changes between these two plots. Figures 7-9 show the maximum temperature differences between each pair of functions.

One might expect for the two constant D value function and the hyperbolic tangent function to contain the largest temperature difference due to the number of refinements made to reach the hyperbolic case. However, as can be seen in Table 5, the maximum temperature difference, calculated from the center temperature to the outer ring corresponding to the outer boundary of the cake, occurs between the two constant D and linear cases.

D Range	Figure 1	Figure 2	Figure 3
$D(3)$	18°F	11°F	7°F
$D(2)$	17°F	9°F	7.5°F
$D(1)$	19°F	13°F	6°F

Table 7: Maximum temperature difference (to the nearest °F) between diffusion functions given their corresponding contour plots and range of D values associated with each function respectively.

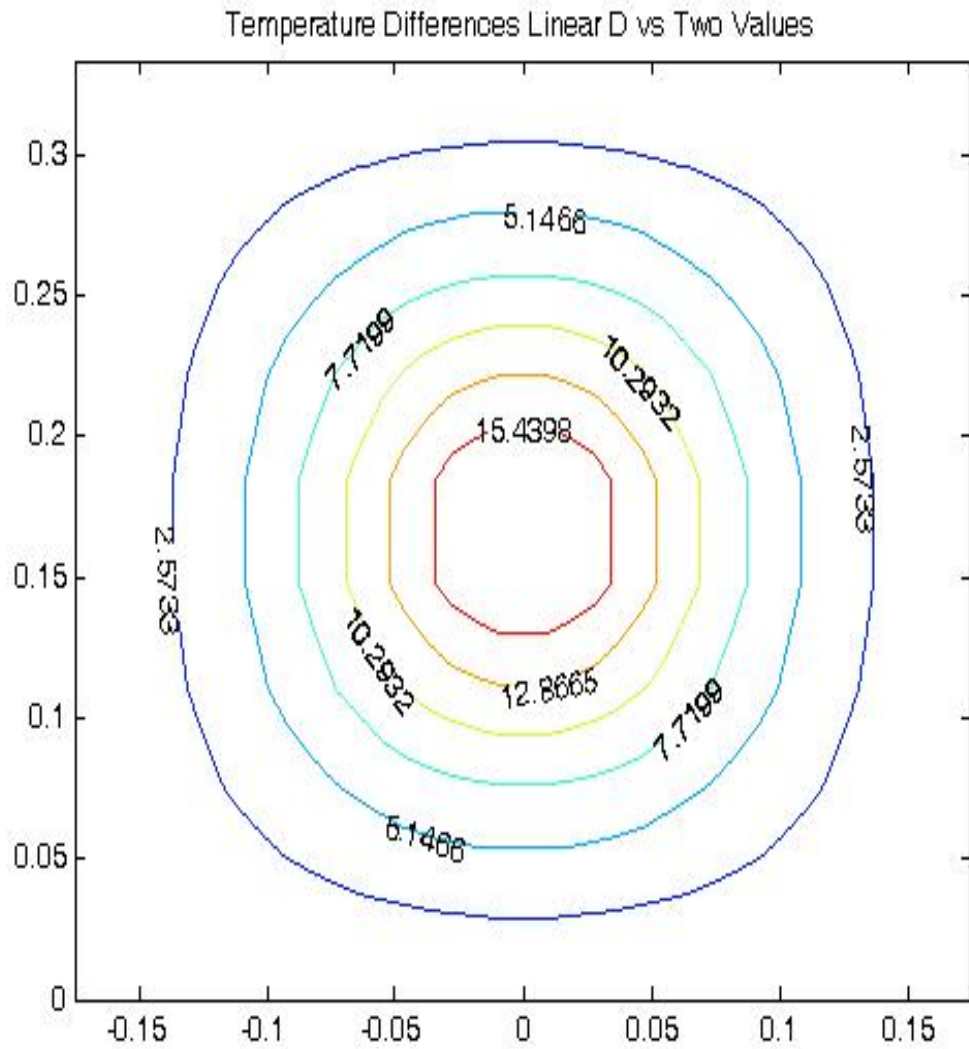


Figure 12: Temperature differences between two D and linear models. Height vertical and radius horizontal are shown in feet.

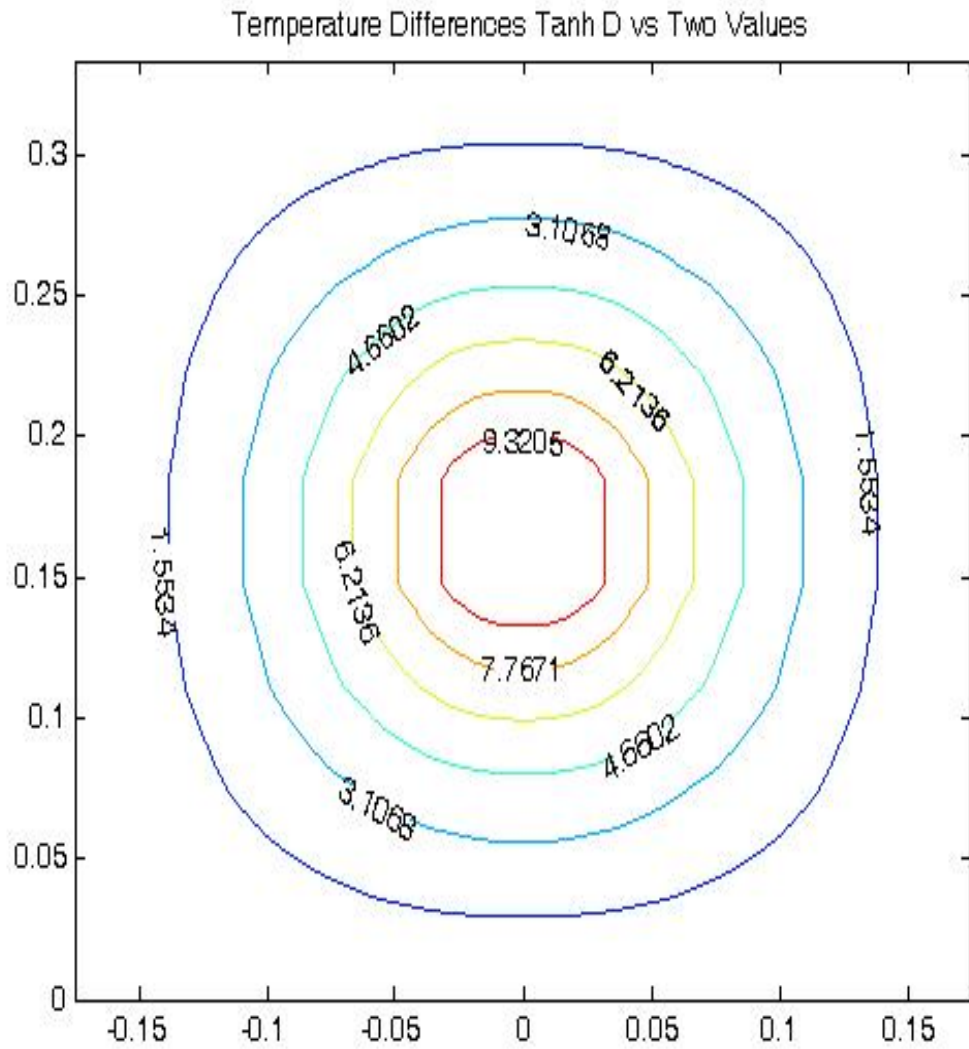


Figure 13: Temperature differences between two D and hyperbolic models. Height vertical and radius horizontal are shown in feet.

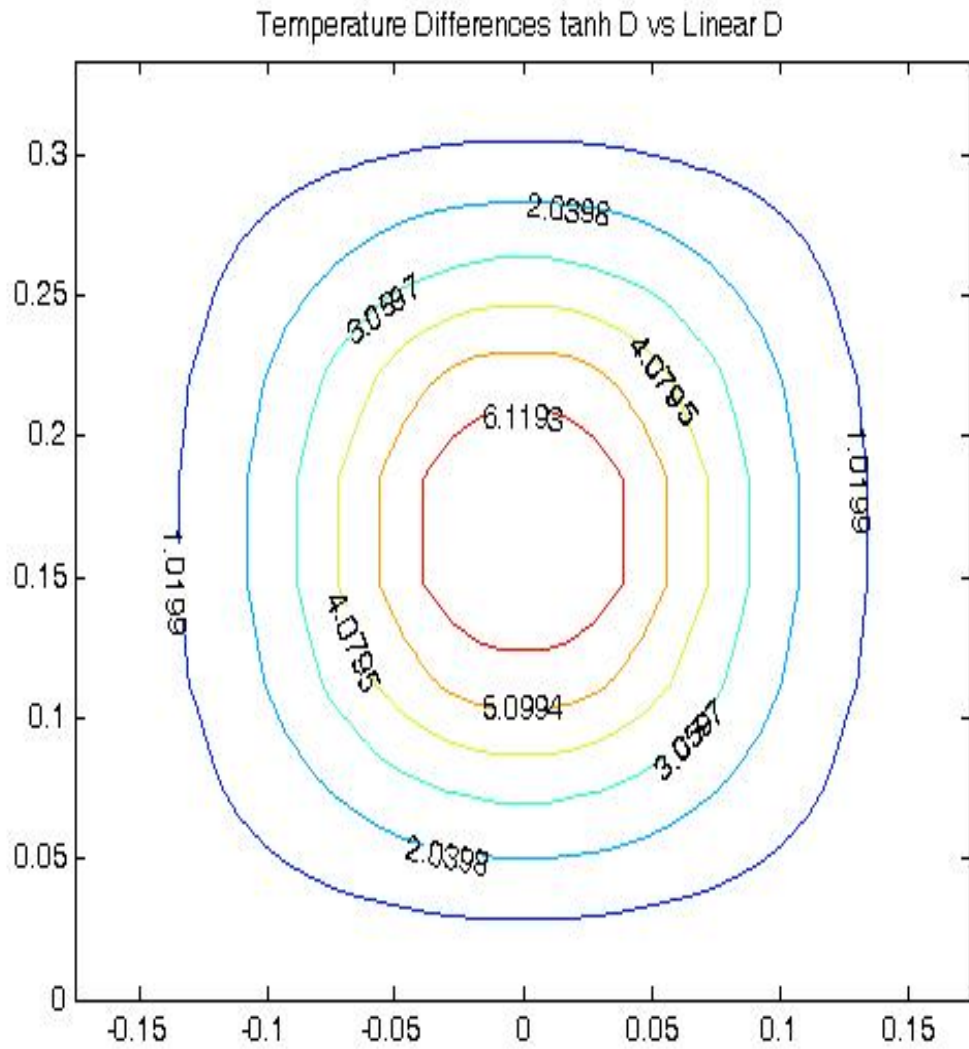


Figure 14: Temperature differences between linear and hyperbolic models. Height vertical and radius horizontal are shown in feet.

6 CONCLUSIONS

After initially assuming that heat diffuses at a constant rate throughout the baking process, we realized that this theory does not take into account the different diffusion rates of the different consistencies that form as the batter heats. However, we generally stated that similar cakes (those of equal height or ratio) have similar diffusion rates. From this basis we expanded our search to incorporate the changing diffusions of the varying consistencies. Beginning with the two constant D case, we found a suitable range of D values that satisfied the given dimensions and baking time to reach the desired center temperature of 203°F . We determined this case to be equally unrealistic in that it assumes the batter is either moist or dry and that each diffuses at a rate of D_1 or $D_2 \text{ ft}^2/\text{min}$, respectively. However, we know that the batter changes continuously as it heats and therefore so should its rate of diffusion.

Thus we refined our results and looked at a linear approximation of the rate of diffusion instead. Here we also determined an adequate range of diffusion, but once again our model failed to incorporate the continuing change of diffusion of batters which reach temperatures greater than 212°F , at which point the moisture in the batter was determined to evaporate. To incorporate this change, we again wished to smooth the transition from the greater diffusion of the initial moist batter to the lesser diffusion of the drier batter. We found a hyperbolic tangent curve to complement our linear approximation and determined that this model best suited the ever changing diffusion that takes place throughout the baking process. Comparing the three models, we found that the two constant D and hyperbolic tangent cases showed the least temperature difference, thus the greatest similarities.

Apart from our focus on determining non-constant diffusion rates, Dr. Olaszewski's initial goal of determining these rates in order to predict baking times [2] was also taken into consideration. Various runs using the dimensions from

Cakes 2 and 3 were made to see if the baking times could be predicted relatively accurately using our three models, the hyperbolic tangent curve in particular. Center temperatures were evaluated at the expected baking times for the specified cakes but on various occasions this resulted in an excess of 300°F when using the range of diffusion rates found for our three models. These findings were concluded to be due to the fact that Cake 1 was used to determine the diffusion ranges for all three models and has been shown to have the highest rate of diffusion. Noting that the lowest range of diffusion values (found for the two constant D case) yielded the lowest center temperature during our trial process, we leave room for future work to investigate whether or not using one of the mid-range, constant D cakes could then be used to find similar diffusion ranges and then be applied to predict similar baking times.

Future work is also left to explore our initial model using the heat equation without the assumption that density and specific heat depend solely on spatial direction but also time dependent and not approximately constant. Also, one could vary the boundary conditions from the fixed case we assumed and instead consider mixed conditions which would take into account that heat does not always flow in a single direction. This being said, many alternate routes could be taken to determine the effects of conduction, convection, and radiation which are also not taken into account with our model. An extensive system of partial differential equations would be needed to incorporate the many intricate factors and processes which take place during the baking process.

On top of the already mentioned, other topics to be explored include: incorporating the conductivity of various baking pans, conduction vs. convection ovens, the moisture content of various recipes, cupcakes, angel food cake (which we previously mentioned would require Bessel equations of the second kind), and many other branches into the numerous applications of the baking process.

REFERENCES

- [1] Zanoni, Pierucci and Peri, *Study of the Bread Baking Process - II Mathematical Modeling*. J. Food Eng. 23, 1994.
- [2] Olszewski, *From Baking a Cake to Solving the Diffusion Equation*. American Journal of Physics, June 2006.
- [3] von Winckel, Greg, *besselzero.m*, Jan. 2005.
- [4] “A Guide to MATLAB.” *Numerical Solutions of the Heat Equation*. Oct 2007.
<http://www.math.umd.edu/undergraduate/schol/matlab/pde.doc>.
- [5] Haberman, *Applied Partial Differential Equations with Fourier Series and Boundary Value Problems*. 4th ed. Pearson: Prentice Hall, 2004.

APPENDIX

A. Diffusion

Determination of a diffusion constant given the cake size and known baking time to reach a center temperature of 203°F.

```
%Temperatures
Ti=80;
Tb=350;
%Cake dimensions (in feet)
a=2.1/12;
H=4/12;
%Point of evaluation
r=0;
z=H/2;
%Baking time
t=26;
%Number of terms
N=1000;
M=1000;
n=1:N;
m=1:M;
%Evaluate zeros of Bessel functions
j0=besselzero(0,M,1);
j1=j0.*besselj(1,j0);
%Set up arrays
S=sin((2*n-1)*pi*z/H)./(2*n-1);
B=besselj(0,r/a*j0(m))./(j1(m));
%Diffusion constant
D=17.9073e-5;
for j=1:10
    D=D+j*(1.0e-8);
    E1=exp(-((2*n-1)*pi/H).^2*D*t);
    E2=exp(-(j0(m)/a).^2*D*t);
    u(j)=Tb+8*(Ti-Tb)/pi*B'*E2*E1*S';
    d(j)=D;
end
plot(d,u,'x')
title('Temperature at Center vs Diffusion Constant')
xlabel('Diffusion Constant (ft^2/min)')
ylabel('Temperature (F)')
```

B. Besselzeros

Called in diffusion.m to find the first k zeros of the Bessel function $J(n,x)$.

```
function x=besselzero(n,k,kind)

k3=3*k;
x=zeros(k3,1);
for j=1:k3
    % Initial guess of zeros
    x0=1+sqrt(2)+(j-1)*pi+n+n^0.4;

    % Do Halley's method
    x(j)=findzero(n,x0,kind);

    if x(j)==inf
        error('Bad guess. ');
    end
end

x=sort(x);
dx=[1;abs(diff(x))];
x=x(dx>1e-8);
x=x(1:k);
function x=findzero(n,x0,kind)
n1=n+1;    n2=n*n;

% Tolerance
tol=1e-12;

% Maximum number of times to iterate
MAXIT=100;

% Initial error
err=1;
iter=0;
while abs(err)>tol & iter<MAXIT
    switch kind
        case 1
            a=besselj(n,x0);
            b=besselj(n1,x0);
        case 2
            a=bessely(n,x0);
            b=bessely(n1,x0);
    end
end
```

```
x02=x0*x0;
err=2*a*x0*(n*a-b*x0)/(2*b*b*x02-a*b*x0*(4*n+1)+(n*n1+x02)*a*a);
x=x0-err;
x0=x;
iter=iter+1;
end

if iter>MAXIT-1
    warning('Failed to converge to within tolerance. ',...
           'Try a different initial guess');
    x=inf;
end
```

C. Numerical Solutions

I. Finite Difference Scheme - *heatcylf.m*

Solution of Heat Equation in cylindrical coordinates with Dirichlet BCs using explicit finite difference scheme.

```
function u = heatcylf(D1, D2, t, r, z, init, bdry,alpha)
% Solution of Heat Equation in cylindrical coordinates
% with Dirichlet BCs using explicit finite difference

K = length(r);
M = length(z);
N = length(t);
dr = mean(diff(r));
dz = mean(diff(z));
dt = mean(diff(t));

u = zeros(N,K,M);
u(1, :, :) = init;
D=D1*ones(size(init));
for n = 1:N-1
    for i=2:K-1
        for j=2:M-1
            % Diffusion Terms
            Dur(i,j) = u(n,i-1,j)*(D(i-1,j)*r(i)+ 2*D(i,j)*(r(i-1)+ r(i))
                                -D(i+1,j)*r(i))/4/dr^2 ...
                - 2*u(n,i,j)*D(i,j)*r(i)/dr^2 ...
                - u(n,i+1,j)*(D(i-1,j)*r(i)-2*D(i,j)*(r(i)+r(i+1))
                                -D(i+1,j)*r(i))/4/dr^2;
            Duz(i,j) = u(n,i,j-1)*(D(i,j-1)+4*D(i,j)-D(i,j+1))/4/dz^2 ...
                - 2*u(n,i,j)*D(i,j)/dz^2 ...
                - u(n,i,j+1)*(D(i,j-1)-4*D(i,j)-D(i,j+1))/4/dz^2;

            u(n+1,i,j) = u(n,i,j) + dt*(Dur(i,j)/r(i)+Duz(i,j));
        end
    end
end
% Boundary Conditions
u(n+1,K,2:M-1) = bdry(1);
u(n+1,2:K-1,1) = bdry(2);
u(n+1,2:K-1,M) = bdry(3);
%u(n+1,1,2:M-1) = bdry(4);
u(n+1,1,2:M-1) = u(n,2,2:M-1);
```

```

    % Diffusion Matrix
    U(:,:)=u(n,,:);
    D=heatD(D1,D2,U,alpha);
end

```

II. Contour Solution Plots - *heatFDcyl.m*

Inputs the given cake dimensions and diffusion values into *heatcylf.m* and plots vertical slices taken at the center of the cake at the specified times given by Tmax. For the dimensions listed below, the center of the cake should be $\approx 203^\circ\text{F}$ at Tmax=26.

```

clear
for alpha=1:3
    figure(alpha)
    N=3000;
    K=20;
    M=10;
    R=2.1/12;
    H=4/12;
    Tmax = [12; 18; 23; 26];
    minT=80;
    maxT=350;
    %alpha=1
    %D2=19e-5;
    %D1=16e-5;

    %alpha=2
    %D2=15.2e-5;
    %D1=20.0e-5;

    %alpha=3
    D2=16.3e-5;
    D1=23e-5;
    for k = 1:length(Tmax)
        tvals = linspace(0, Tmax(k), N);
        rvals = linspace(0, R, K);
        zvals = linspace(0, H, M);
        init = (80-350)*ones(K,M);
        uvals = 350 + heatcylf(D1, D2, tvals, rvals, zvals, init, [0,0,0,0],alpha);
        U(1:K,1:M) = uvals(N-1,:,:);

        for i=1:K
            C(i+K-1,1:M) = U(i,1:M);

```

```

        C(K+1-i,1:M) = U(i,1:M);
        rr(K+1-i) = -rvals(i);
        rr(i+K-1) = rvals(i);
    end
    %figure
    subplot(2,2,k)
    contourLevels = [80:20:350];
    [c,h] = contourf(rr,zvals,C',contourLevels); colorbar
    set(gca, 'CLim', [minT, maxT]);
    title(['Temeratures for t= ' num2str(Tmax(k)) ' min'])
end
    if alpha==1
        C1=C;
    elseif alpha==2
        C2=C;
    else
        C3=C;
    end
end
figure(4)
[c,h] = contour(rr,zvals,abs(C2-C1)',6);
clabel(c,h,'manual');
set(gca, 'CLim', [0, max(max(abs(C2-C1)))]);
title(['Temerature Differences Linear D vs Two Values'])

figure(5)
[c,h] = contour(rr,zvals,abs(C3-C1)',6);
clabel(c,h,'manual');
set(gca, 'CLim', [0, max(max(abs(C3-C1)))]);
title(['Temerature Differences Tanh D vs Two Values'])

figure(6)
[c,h] = contour(rr,zvals,abs(C3-C2)',6);
set(gca, 'CLim', [0, max(max(abs(C3-C2)))]);
clabel(c,h,'manual');
title(['Temerature Differences tanh D vs Linear D'])
[max(max(abs(C2-C1))) max(max(abs(C3-C1))) max(max(abs(C3-C2)))] ]

```

III. Diffusion Functions Defined - *heatD.m*

Called in *heatcylf.m* to be input as the diffusion matrix given $\alpha = 1 : 3$, *heatD.m* defines each derived diffusion function in Chapter 5 for their specific values and constraints.

```

function d = heatD(D1, D2, temp,alpha)
[k,m]=size(temp);
% Initialized constants
a=(D1-D2)/2;
b=(D1+D2)/2;
%c=1;
%c=25;
%c=50;
%c=75;
%c=100;
c=132;
T1=80-350;
T2=212-350;
T3=T2-c;
T4=(T2+T3)/2;
TT=2*(temp-T4)/(D1-D2);
% Slopes
beta=(D1-D2)/(T3-T2);
if alpha==1
% Function for two constant values D1>=D2
for i=1:k
    for j=1:m
        if temp(i,j)>T2
            d(i,j)=D2;
        else
            d(i,j)=D1;
        end
    end
end
elseif alpha==2
    % Function for a linear ramp of slope beta through (T4,(D1+D2)/2)
for i=1:k
    for j=1:m
        if temp(i,j)>T4
            d(i,j)=D2;
        elseif temp(i,j)<T3
            d(i,j)=D1;
        else
            d(i,j)=beta*(temp(i,j)-T4)+b;
        end
    end
end
elseif alpha==3
    % Function for a smooth ramp of slope beta through (T4,(D1+D2)/2)

```

```
end      d=a*tanh(beta*TT)+b;
```

D. Non-Constant Plots

Plots linear and hyperbolic tangent curves given temperature and D value range.

```
% Routine to plot piecewise linear and tanh ramps
% for varying diffusion ranges
%
T=linspace(-270,0,100);
% Diffusion Constants with D1>D2
%alpha=1
%D2=19e-5;
%D1=16e-5;

%alpha=2
%D2=15.2e-5;
%D1=20.0e-5;

%alpha=3
D2=16.3e-5;
D1=23e-5;
% Initialized constants
a=(D1-D2)/2;
b=(D1+D2)/2;
c=132;
T1=80-350;
T2=212-350;
T3=T2-c;
T4=(T2+T3)/2;
TT=2*(T-T4)/(D1-D2);
% Plot smooth ramp of slope beta through (T4,(D1+D2)/2)
    beta=(D1-D2)/(T3-T2);
    f=a*tanh(beta*TT)+b;
    hold
    plot(T+350,f)
    hold
% Plot linear ramp of slope beta through (T4,(D1+D2)/2)
    for i=1:100
        if T(i)>T2
            d(i)=D2;
        elseif T(i)<T3
            d(i)=D1;
        else
            d(i)=beta*(T(i)-T4)+b;
        end
    end
end
```

```
hold
plot(T+350,d,'r')
hold
```